Title: Matter-driven phase transition in lattice quantum gravity

Speakers: Andrzej Gorlich

Series: Quantum Gravity

Date: May 06, 2021 - 2:30 PM

URL: http://pirsa.org/21050009

Abstract: The model of Causal Dynamical Triangulations (CDT) is a background-independent and diffeomorphism-invariant approach to quantum gravity,

which provides a lattice regularization of the formal gravitational path integral. The framework does not involve any coordinate system and employs only geometric invariants. For a Universe with toroidal spatial topology, we can introduce coordinates using classical scalar fields with periodic boundary conditions with a jump. The field configurations reveal pictures of cosmic voids and filaments surprisingly similar to the ones observed in the present-day Universe. I will discuss the impact of dynamical matter fields on the geometry of a typical quantum universe in the four-dimensional CDT model and explain several observed phenomena. In particular, a phase transition is triggered by the change of the scalar field jump amplitude. This discovery may have important consequences for quantum universes with non-trivial topology since the phase transition can change the topology to a simply connected one.

 

# Matter-driven phase transition in lattice quantum gravity

Andrzej Görlich

Institute of Theoretical Physics, Jagiellonian University, Poland

*Quantum gravity seminars* at Perimeter Institute

May 6th, 2021

# Introduction to Causal Dynamical Triangulations

## What is Causal Dynamical Triangulations?

*Causal Dynamical Triangulations* is a background independent and diffeomorphism invariant approach to quantum gravity. It provides a lattice regularization of the formal gravitational path integral via a sum over causal triangulations.

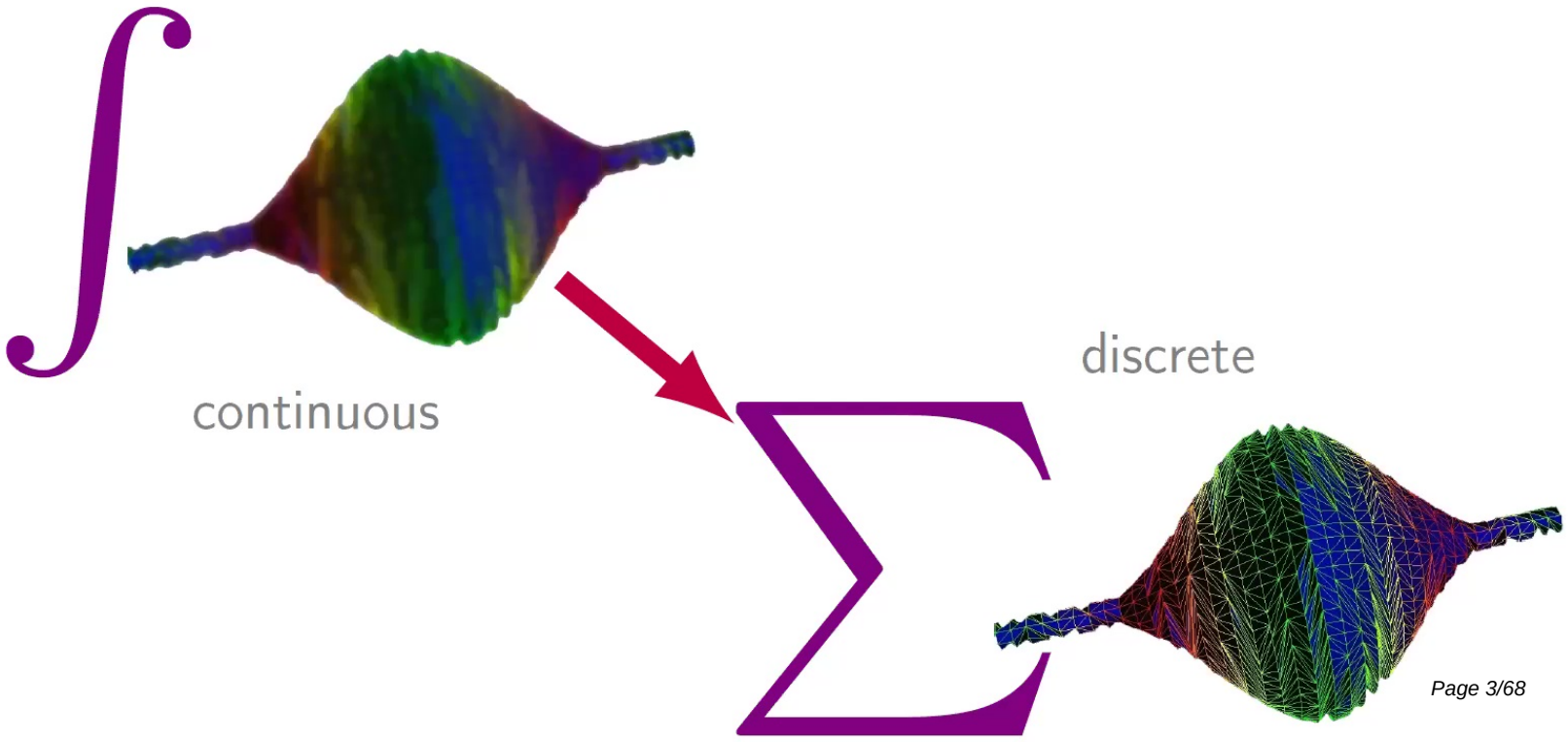

# Discretization

## The partition function

$$\int \mathrm{D}[g] e^{iS^{EH}[g]} \longrightarrow \sum_{\mathcal{T}} e^{-S^{R}[\mathcal{T}]}$$

## The action

The Einstein-Hilbert action has a natural realization on piecewise linear geometries called the Regge action

$$S^{EH}[g] = -\frac{1}{G}\int \mathrm{d}t \int \mathrm{d}^{D}x\sqrt{g}(R - 2\Lambda)$$

$$\downarrow$$

$$S^{R}[\mathcal{T}] = -K_0 N_0 + K_4 N_4 + \Delta(N_{41} - 6N_0)$$

$N_0, N_4, N_{41}$ number of vertices, simplices and $\{4,1\}$-simplices

$K_0, K_4, \Delta$ bare coupling constants $(G, \Lambda, a_t/a_s)$

# Topology and causality in CDT

- **Causal** **D**ynamical **T**riangulations assumes a global proper-time foliation of the spacetime manifold $\mathcal{M} = \Sigma \times S^1$.
- Leaves of the foliation $\Sigma$ (spatial slices) are built of equilateral tetrahedra. The spatial topology is fixed *(controlled)* and is not allowed to change in time *(spherical or toroidal)*.
- Distinction between time-like and spatial-like links.
- Wick rotation $(a_t^2 \to -a_t^2)$.
- Time-periodic boundary conditions are chosen for simplicity.

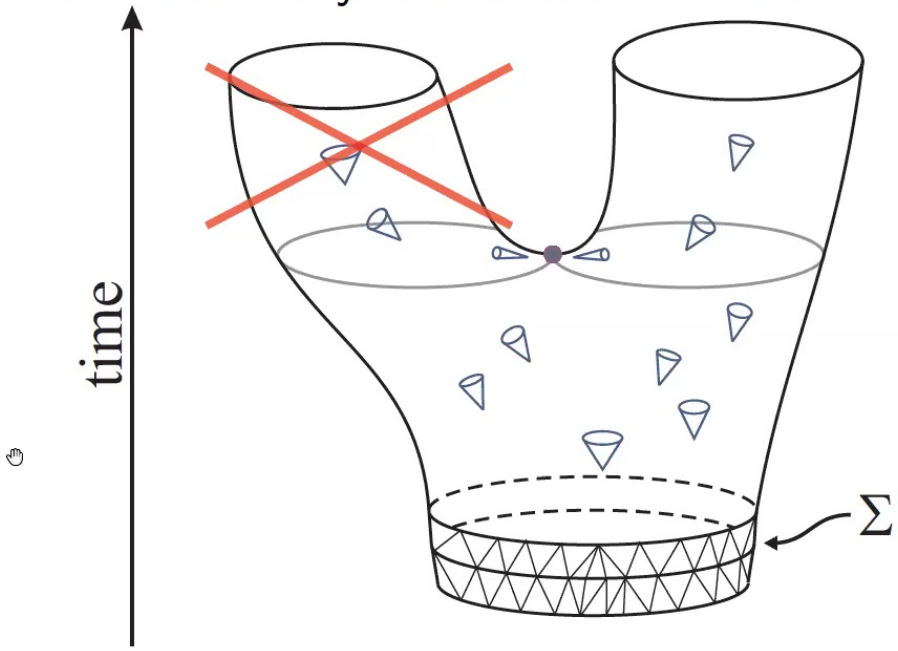

# Fundamental building blocks

Two types of simplices: $\{4,1\}$ and $\{3,2\}$ + mirror reflections.
Simplices connect adjacent slices.

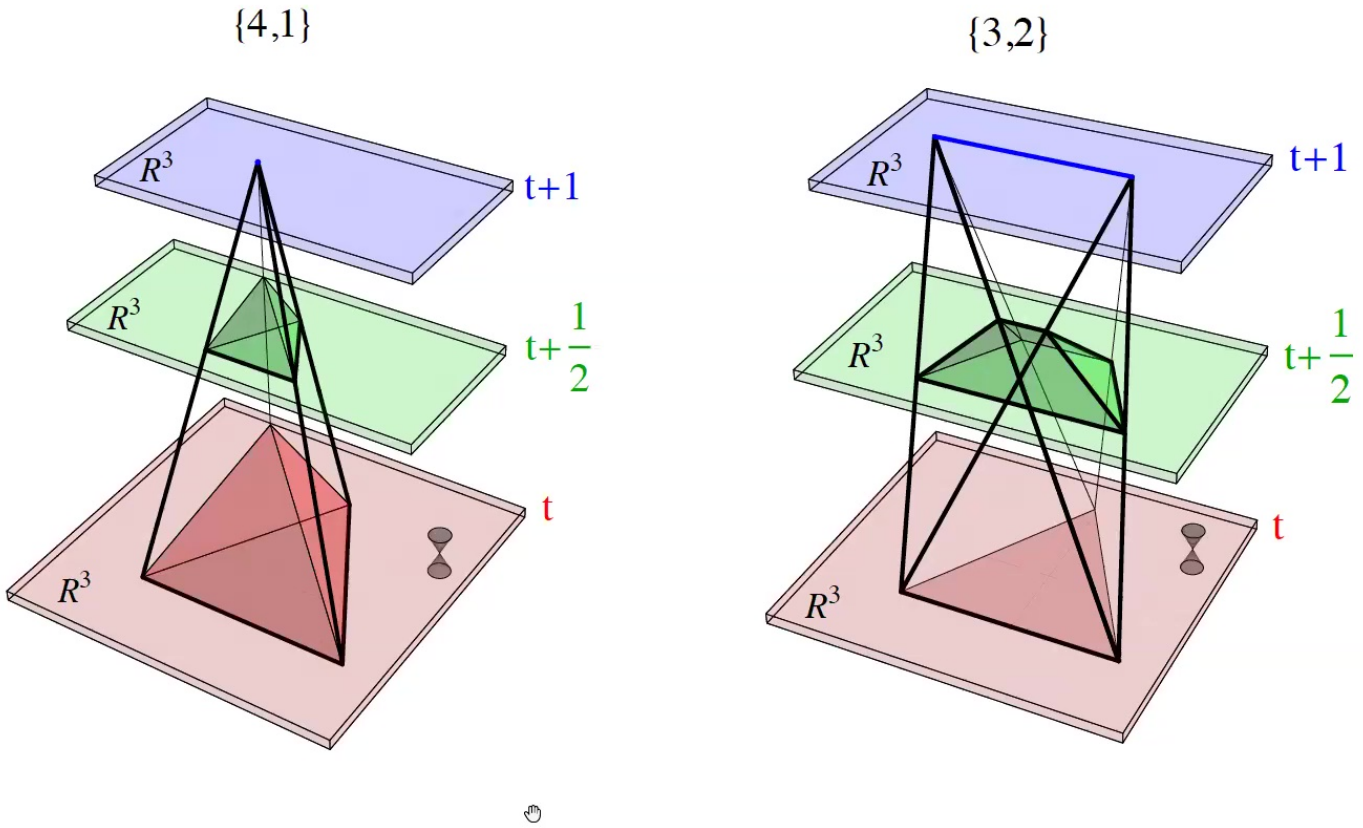

# Fundamental building blocks

Two types of simplices: $\{4, 1\}$ and $\{3, 2\}$ + mirror reflections.
Simplices connect adjacent slices.

# Fundamental building blocks

Two types of simplices: $\{4,1\}$ and $\{3,2\}$ + mirror reflections.
Simplices connect adjacent slices.

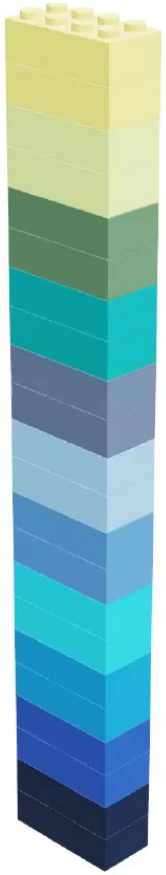

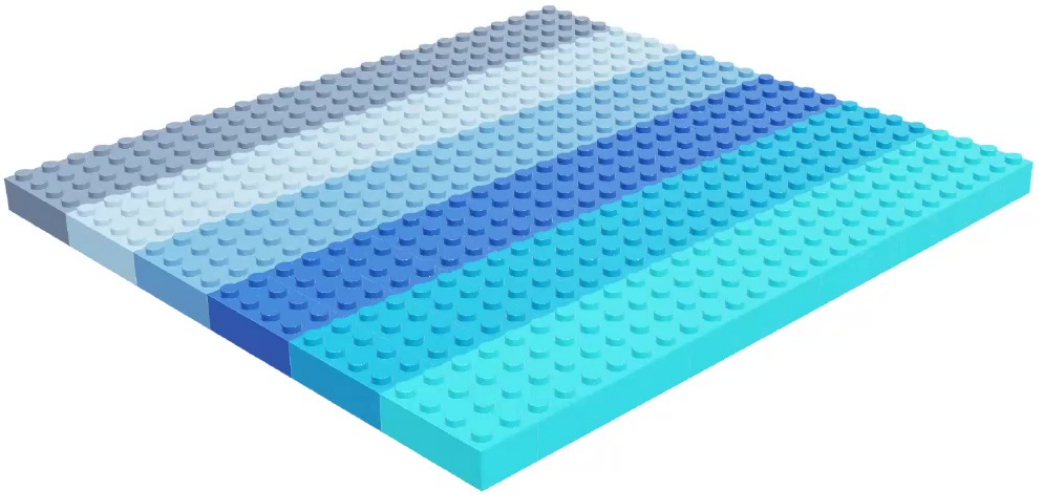

# Fundamental building blocks

Two types of simplices: $\{4,1\}$ and $\{3,2\}$ + mirror reflections.
Simplices connect adjacent slices.

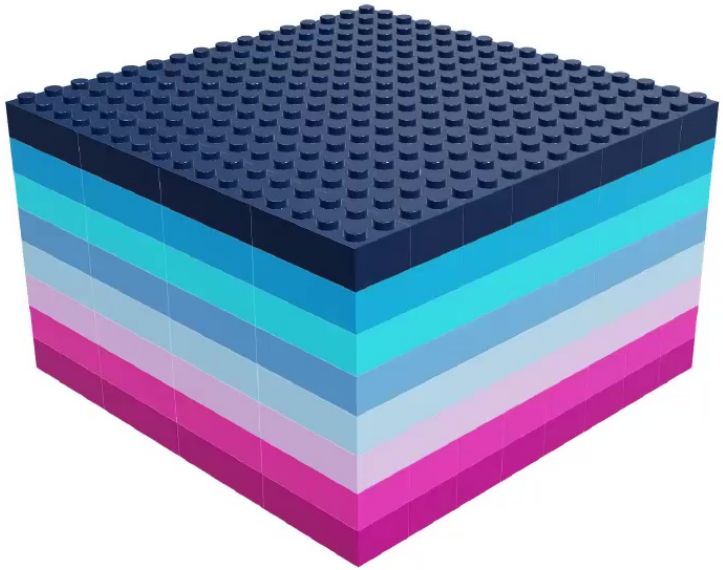

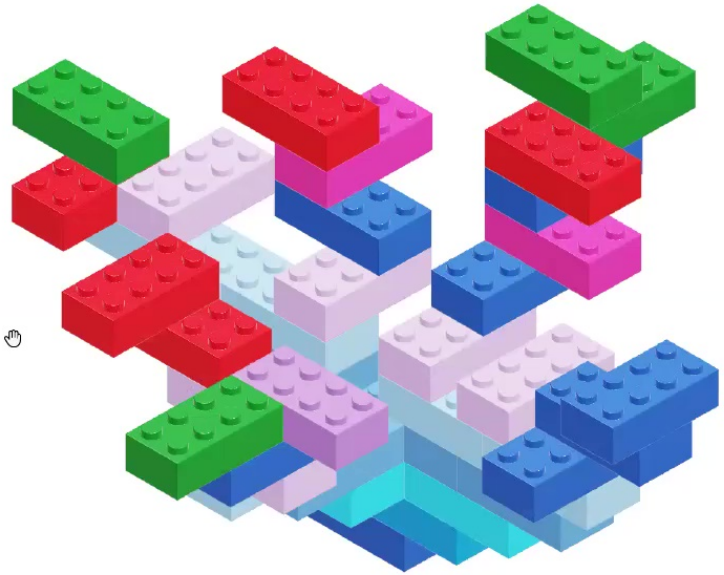

# Monte Carlo simulations

During the simulations, we perform a random walk over the state space.

| | |
|---|---|
| Ergodicity | all possible configurations can be reached |
| Fixed topology | moves do not change the topology |
| Causality | moves preserve the foliation |
| 4D CDT | set of seven types of **Pachner moves** |
| Fixed volume | additional volume fixing term |

## Example of a 2D Monte Carlo move

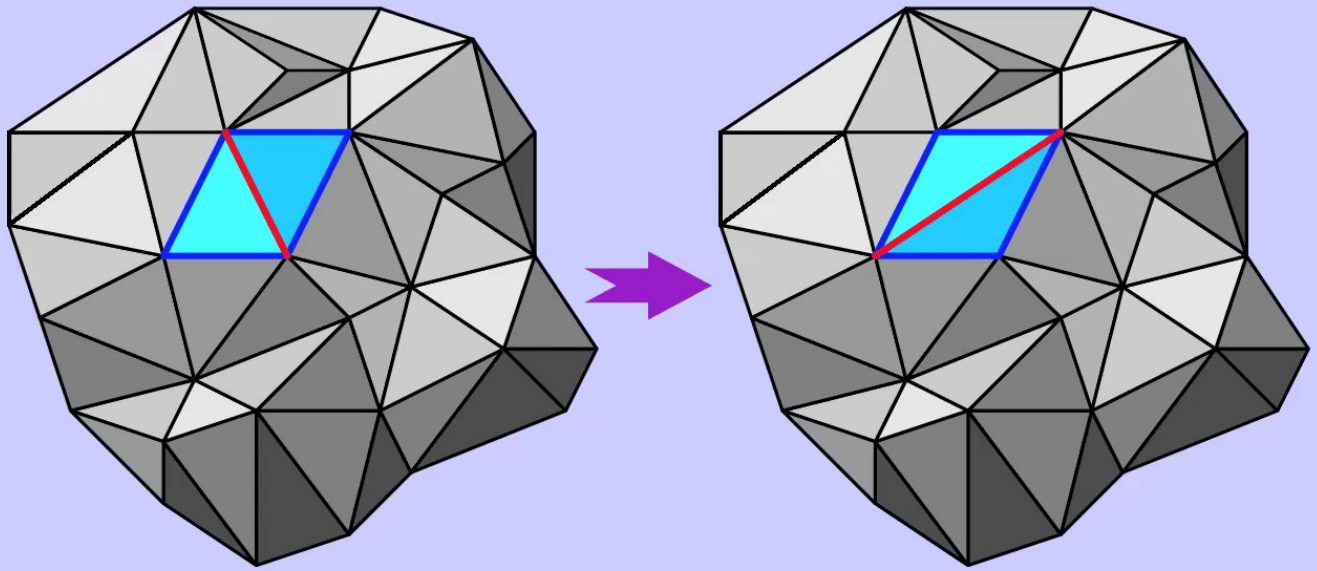

# Monte Carlo simulations

During the simulations, we perform a random walk over the state space.

| | |
|---|---|
| Ergodicity | all possible configurations can be reached |
| Fixed topology | moves do not change the topology |
| Causality | moves preserve the foliation |
| 4D CDT | set of seven types of **Pachner moves** |
| Fixed volume | additional volume fixing term |

## Example of a 2D Monte Carlo move

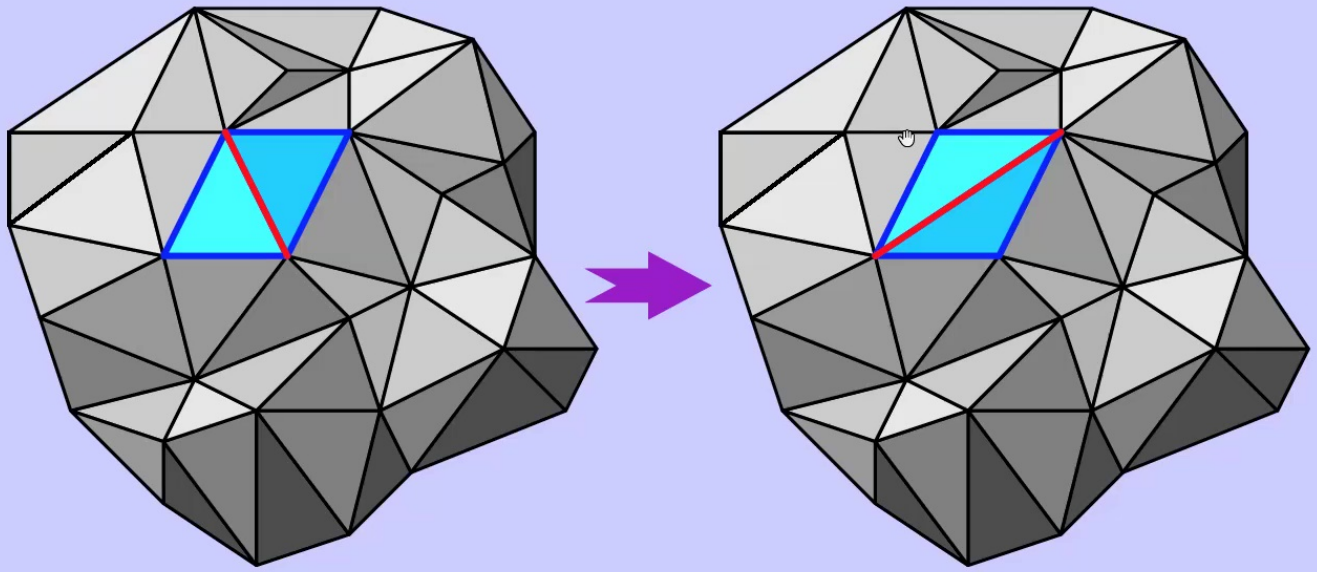

# Coordinates *via* classical scalar fields with a jump

**We can use *classical scalar fields* to define *coordinates***

- For a toroidal topology, we can define four *non-contractible* and *non-equivalent* three-dimensional hypersurfaces.
- For each boundary, we introduce a classical scalar field (non-dynamical) with a jump at the boundary.
- Every simplex is assigned four real numbers $(\varphi^x, \varphi^y, \varphi^z, \varphi^t)$ - values of four scalar fields for the four boundaries $(x, y, z, t)$.
- We use those values as "coordinates" of a simplex .
- The boundary is non-physical and is introduced to stretch the scalar field, thus the classical solution should depend trivially on the boundary.

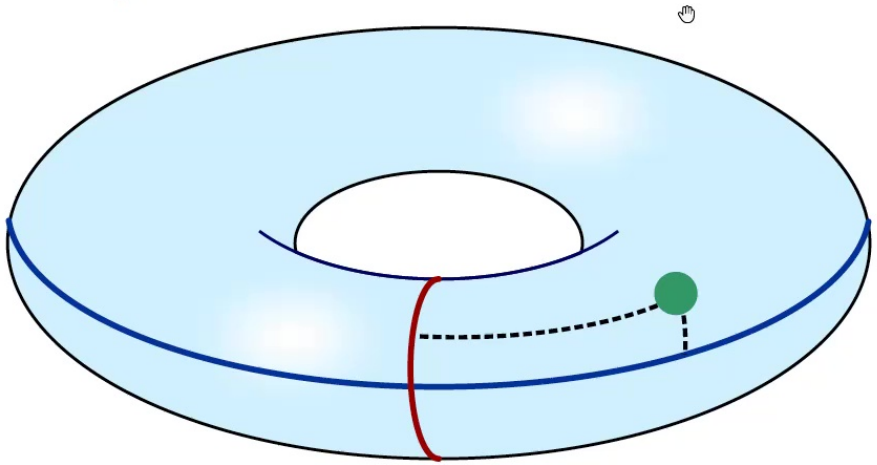

# Coordinates *via* classical scalar fields with a jump

**We can use *classical scalar fields* to define *coordinates***

- For a toroidal topology, we can define four *non-contractible* and *non-equivalent* three-dimensional hypersurfaces.
- For each boundary, we introduce a classical scalar field (non-dynamical) with a jump at the boundary.
- Every simplex is assigned four real numbers $(\varphi^x, \varphi^y, \varphi^z, \varphi^t)$ - values of four scalar fields for the four boundaries $(x, y, z, t)$.
- We use those values as "coordinates" of a simplex .
- The boundary is non-physical and is introduced to stretch the scalar field, thus the classical solution should depend trivially on the boundary.

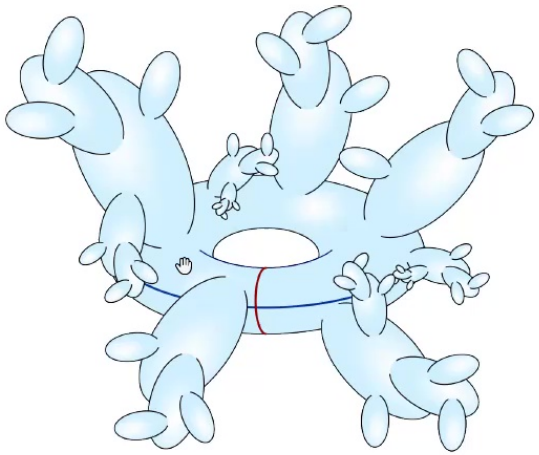

# Classical scalar field with a jump at the boundary

- The action of the free real scalar massless field theory with periodic boundary conditions with a **jump** at the boundary is

$$S[\varphi] = \frac{1}{2}\int \mathrm{d}^4x\,\sqrt{g(x)}\partial_\mu\varphi\partial^\mu\varphi \longrightarrow S[\varphi] = \sum_{i\leftrightarrow j}(\varphi_i - \varphi_j - B_{ij})^2,$$

where B is an antisymmetric *jump matrix*,

$$B_{ij} = \begin{cases} +1 & \text{if } i \to j \text{ crosses the boundary in positive direction,} \\ -1 & \text{if } i \to j \text{ crosses the boundary in negative direction,} \\ 0 & \text{otherwise.} \end{cases}$$

- When crossing a boundary, a simplex *sees* the field value of its neighbor increased or decreased by one *(orientation)*.
- Non-dynamical - has no impact on quantum geometries

# Coordinates via a scalar field with a jump

- The classical solution, which minimizes the action,

$$S[\varphi] = \sum_{i \leftrightarrow j} (\varphi_i - \varphi_j - B_{ij})^2 = \varphi^\top \mathsf{L} \varphi - 2\varphi^\top b + \|\mathsf{B}\|_F^2$$

  is a solution to the discrete Poisson equation

$$\mathsf{L}\varphi = b,$$

  where L is the Laplacian matrix, $b_i = \sum_j B_{ij}$ is a jump vector, and $\|\mathsf{B}\|_F^2 = \sum_{i,j} B_{ij}^2$ is twice the boundary area.
- Solutions transform **trivially** under boundary redefinition.
- The jump *stretches* the scalar field, although not necessarily in $[0, 1]$ interval.

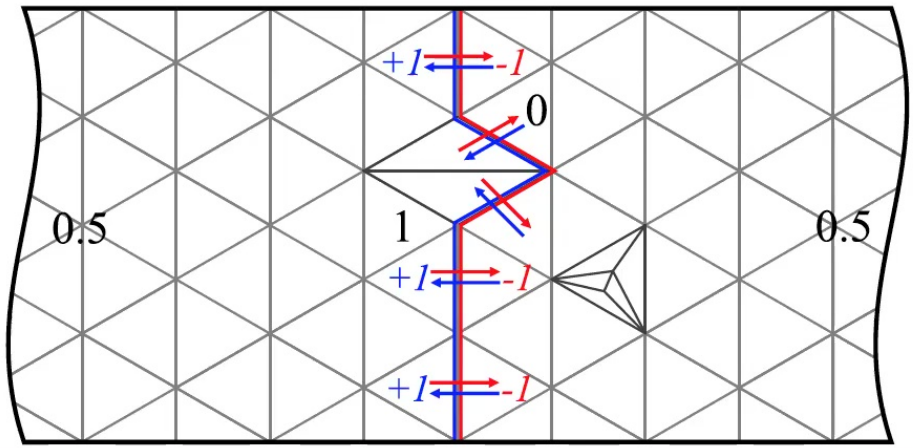

# Coordinates via a scalar field with a jump

- The classical solution, which minimizes the action,

$$S[\varphi] = \sum_{i \leftrightarrow j} (\varphi_i - \varphi_j - B_{ij})^2 = \varphi^\top \mathsf{L} \varphi - 2\varphi^\top b + \|\mathsf{B}\|_F^2$$

  is a solution to the discrete Poisson equation

$$\mathsf{L}\varphi = b,$$

  where L is the Laplacian matrix, $b_i = \sum_j B_{ij}$ is a jump vector, and $\|\mathsf{B}\|_F^2 = \sum_{i,j} B_{ij}^2$ is twice the boundary area.
- Solutions transform **trivially** under boundary redefinition.
- The jump *stretches* the scalar field, although not necessarily in $[0, 1]$ interval.

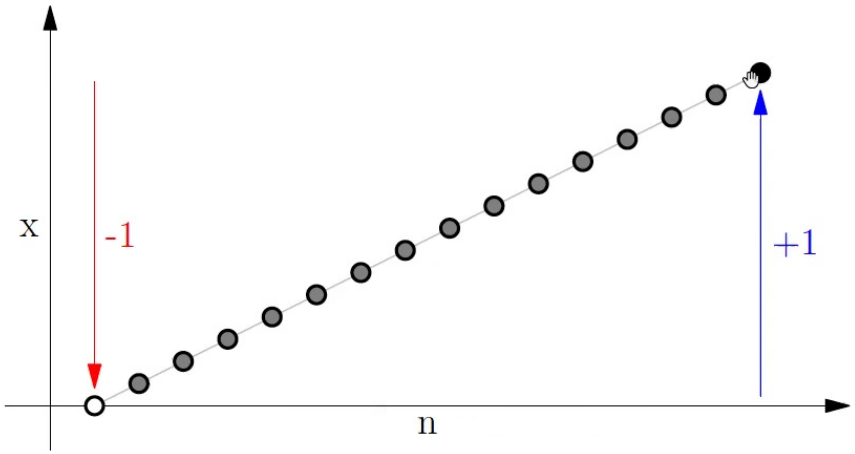

# Coordinates via a scalar field with a jump

- The classical solution, which minimizes the action,

$$S[\varphi] = \sum_{i \leftrightarrow j} (\varphi_i - \varphi_j - B_{ij})^2 = \varphi^\top \mathsf{L} \varphi - 2\varphi^\top b + \|\mathsf{B}\|_F^2$$

  is a solution to the discrete Poisson equation

$$\mathsf{L}\varphi = b,$$

  where L is the Laplacian matrix, $b_i = \sum_j B_{ij}$ is a jump vector, and $\|\mathsf{B}\|_F^2 = \sum_{i,j} B_{ij}^2$ is twice the boundary area.
- Solutions transform **trivially** under boundary redefinition.
- The jump *stretches* the scalar field, although not necessarily in $[0, 1]$ interval.

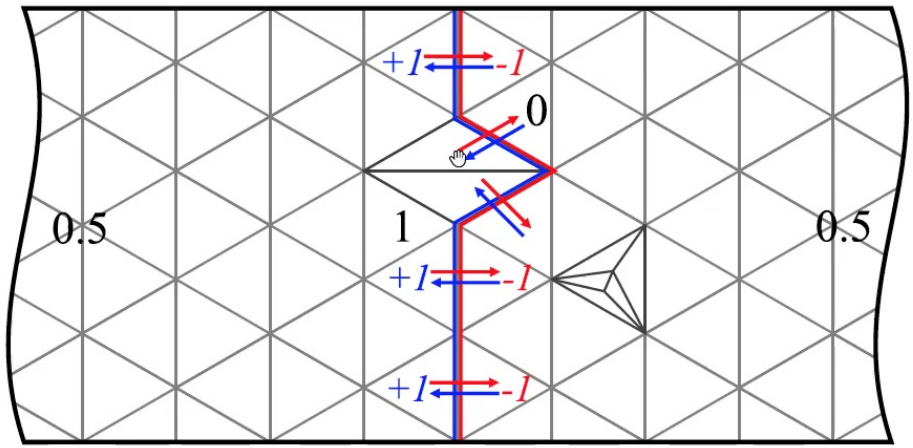

# Classical scalar field with a jump at the boundary

- The action of the free real scalar massless field theory with periodic boundary conditions with a **jump** at the boundary is

$$S[\varphi] = \frac{1}{2}\int \mathrm{d}^4x\,\sqrt{g(x)}\partial_\mu\varphi\partial^\mu\varphi \longrightarrow S[\varphi] = \sum_{i\leftrightarrow j}(\varphi_i - \varphi_j - B_{ij})^2,$$

where B is an antisymmetric *jump matrix*,

$$B_{ij} = \begin{cases} +1 & \text{if } i \to j \text{ crosses the boundary in positive direction,} \\ -1 & \text{if } i \to j \text{ crosses the boundary in negative direction,} \\ 0 & \text{otherwise.} \end{cases}$$

- When crossing a boundary, a simplex *sees* the field value of its neighbor increased or decreased by one *(orientation)*.
- Non-dynamical - has no impact on quantum geometries

# Solving large linear systems

Solving the discrete Poisson equation

$$\mathsf{L}\varphi = b,$$

is a technical problem. The Laplacian matrix is given by

$$\mathsf{L} = 5 \cdot \mathbb{1} - \mathsf{A},$$

where A is the adjacency matrix for a dual triangulation,

$$\mathsf{A} \begin{cases} 1 & \text{if } i \text{ is adjacent to } j, \end{cases}$$

## Coordinates via distances

We used both *direct* and *iterative* methods to solve the discrete Poisson equation.

**Direct** Cholesky decomposition - via `CHOLMOD` library.

**Iterative** **Parallel preconditioned conjugate gradient method with symmetric successive over-relaxation and approximate inverse** - own implementation using `OpenMP`.

a positive constant is added to $\mathsf{L}_{11}$ fixing $\varphi_1 = 0$.

# Solving large linear systems

Solving the discrete Poisson equation

$$\mathsf{L}\varphi = b,$$

is a technical problem. The Laplacian matrix is given by

$$\mathsf{L} = 5 \cdot \mathbb{1} - \mathsf{A},$$

where A is the adjacency matrix for a dual triangulation,

$$\mathsf{A}_{ij} = \begin{cases} 1 & \text{if } i \text{ is adjacent to } j, \\ 0 & \text{otherwise.} \end{cases}$$

- The adjacency matrix and the Laplacian matrix are large ($10^6 \times 10^6$) and sparse matrices ($6 \cdot N$ non-zero elements).
- Up to the (single) zero mode, the Laplacian matrix is a real positive-definite symmetric matrix. To remove the zero mode

$$\sum_{i,j} \mathsf{L}_{ij} = 0 \text{ and } \sum_{i,j} \mathsf{B}_{ij} = 0$$

a positive constant is added to $\mathsf{L}_{11}$ fixing $\varphi_1 = 0$.

# Boundary redefinition

- In general, a solution is not contained withing $[0, 1]$ range.
- It is possible to perform a continuous transformation of a boundary, so that the solution interpolates between 0 and 1.
- For periodic boundary conditions with a jump at the boundary, the solutions are **invariant** under the boundary redefinition up to ***shift modulo-one***. Solutions for two equivalent boundaries belong to the same equivalence class.
- Yet, **the field values are stretched over a given range**.
- Flipping a simplex on the other side of the boundary changes the field value by 1. Mapping of solutions with different boundaries is trivial.

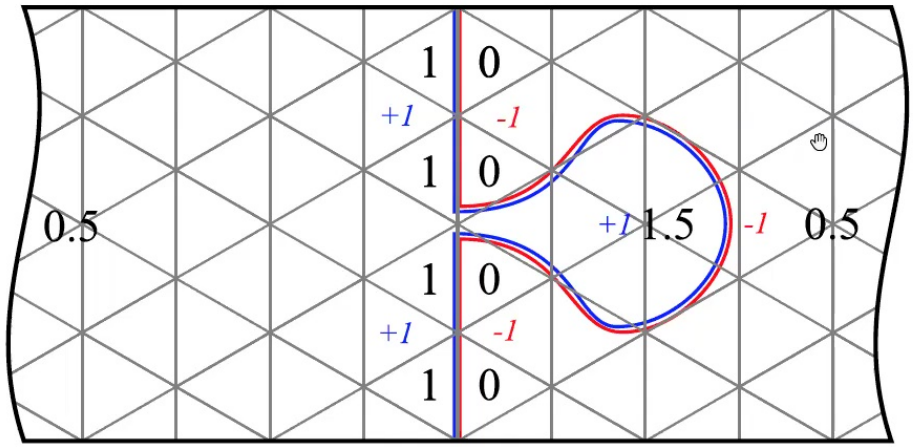

# Boundary redefinition

- In general, a solution is not contained withing $[0, 1]$ range.
- It is possible to perform a continuous transformation of a boundary, so that the solution interpolates between 0 and 1.
- For periodic boundary conditions with a jump at the boundary, the solutions are **invariant** under the boundary redefinition up to ***shift modulo-one***. Solutions for two equivalent boundaries belong to the same equivalence class.
- Yet, **the field values are stretched over a given range**.
- Flipping a simplex on the other side of the boundary changes the field value by 1. Mapping of solutions with different boundaries is trivial.

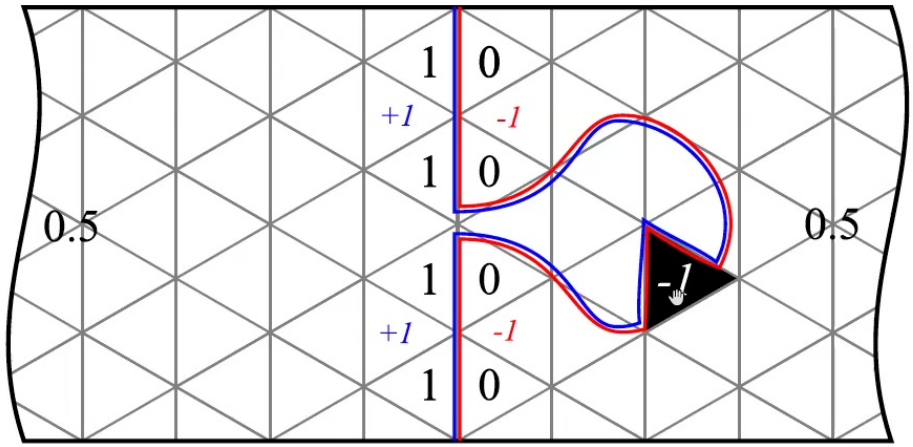

# Coordinates via a scalar field with a jump

- The classical solution, which minimizes the action,

$$S[\varphi] = \sum_{i \leftrightarrow j} (\varphi_i - \varphi_j - B_{ij})^2 = \varphi^\top \mathsf{L} \varphi - 2\varphi^\top b + \|\mathsf{B}\|_F^2$$

  is a solution to the discrete Poisson equation

$$\mathsf{L}\varphi = b,$$

  where L is the Laplacian matrix, $b_i = \sum_j B_{ij}$ is a jump vector, and $\|\mathsf{B}\|_F^2 = \sum_{i,j} B_{ij}^2$ is twice the boundary area.
- Solutions transform **trivially** under boundary redefinition.
- The jump *stretches* the scalar field, although not necessarily in $[0, 1]$ interval.

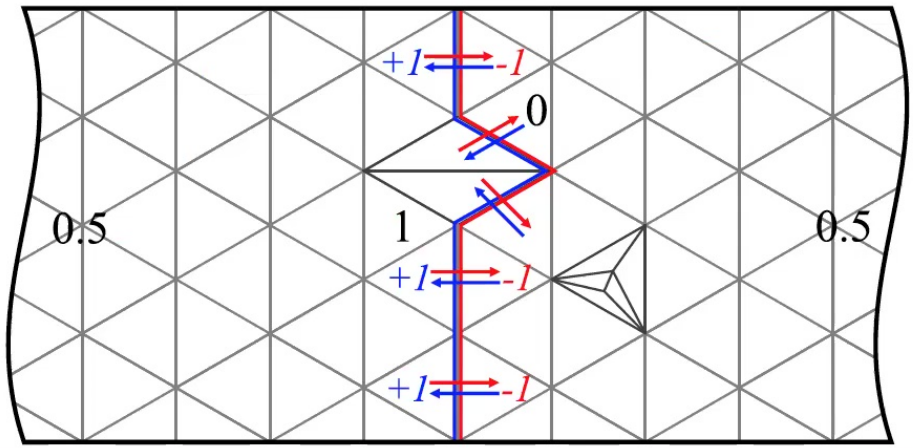

# Boundary redefinition

- In general, a solution is not contained withing $[0, 1]$ range.
- It is possible to perform a continuous transformation of a boundary, so that the solution interpolates between 0 and 1.
- For periodic boundary conditions with a jump at the boundary, the solutions are **invariant** under the boundary redefinition up to ***shift modulo-one***. Solutions for two equivalent boundaries belong to the same equivalence class.
- Yet, **the field values are stretched over a given range**.
- Flipping a simplex on the other side of the boundary changes the field value by 1. Mapping of solutions with different boundaries is trivial.

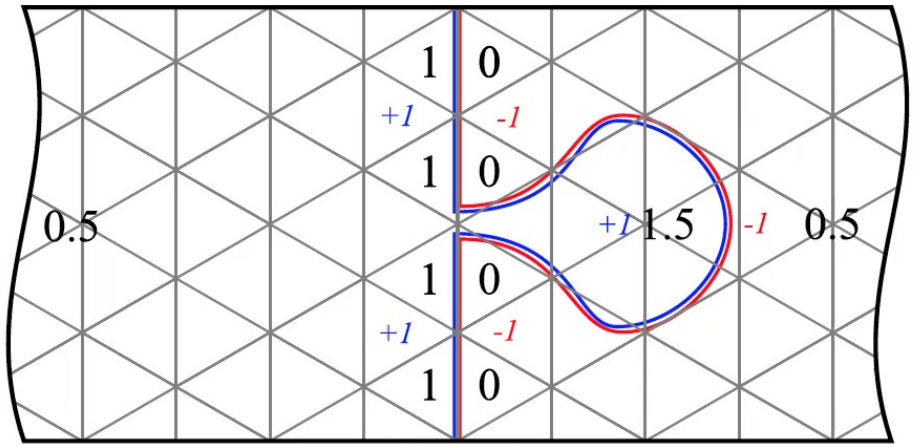

# Boundary redefinition

- In general, a solution is not contained withing $[0, 1]$ range.
- It is possible to perform a continuous transformation of a boundary, so that the solution interpolates between 0 and 1.
- For periodic boundary conditions with a jump at the boundary, the solutions are **invariant** under the boundary redefinition up to ***shift modulo-one***. Solutions for two equivalent boundaries belong to the same equivalence class.
- Yet, **the field values are stretched over a given range**.
- Flipping a simplex on the other side of the boundary changes the field value by 1. Mapping of solutions with different boundaries is trivial.

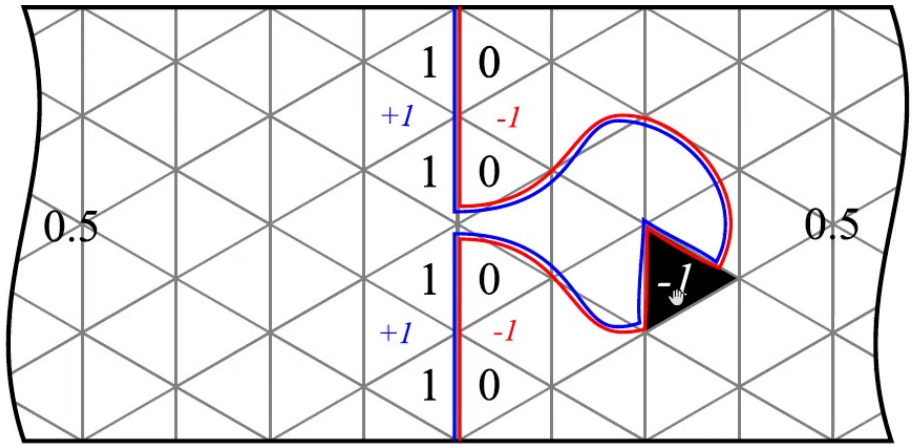

# De Sitter phase ($C_{dS}$)

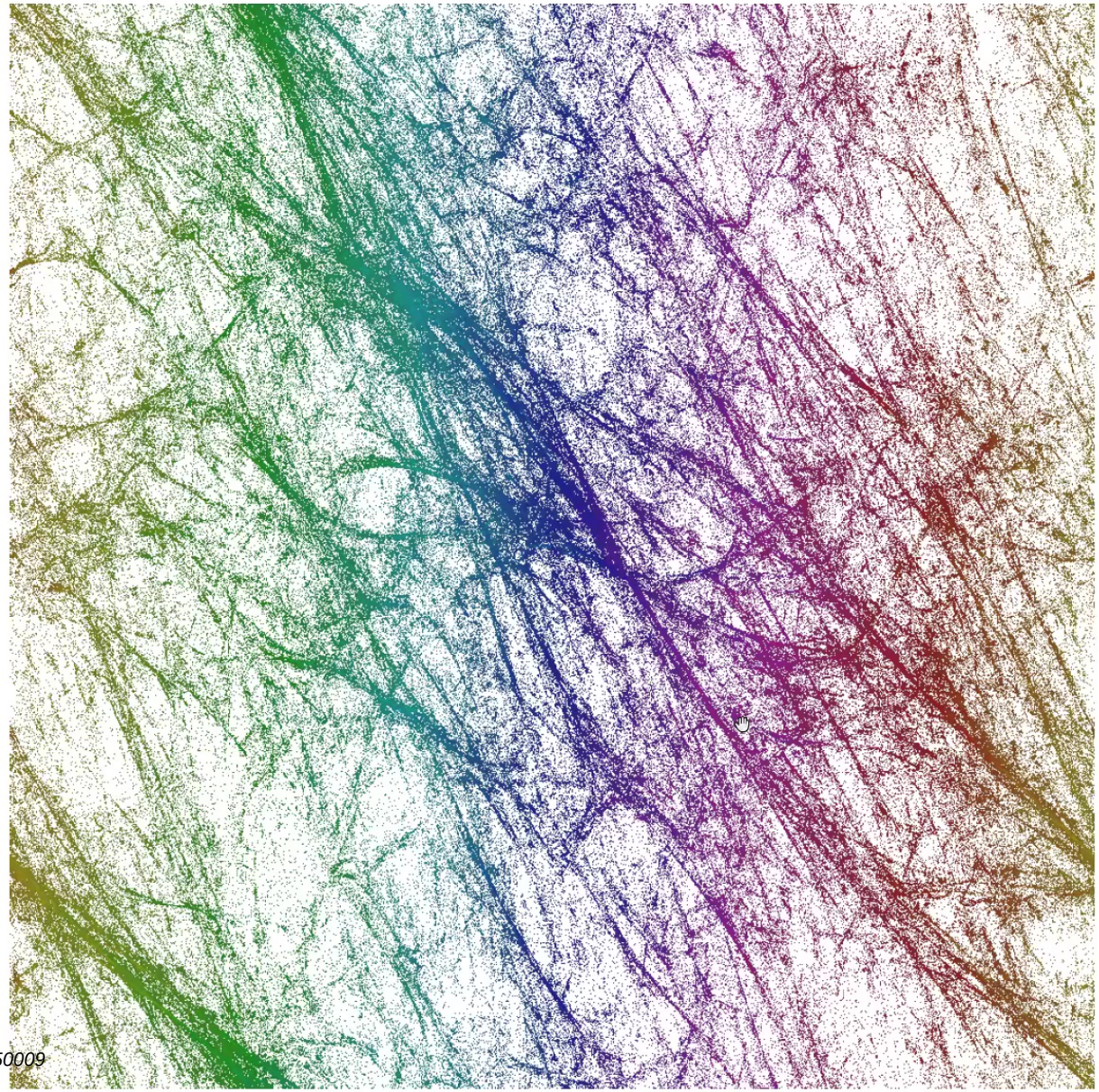

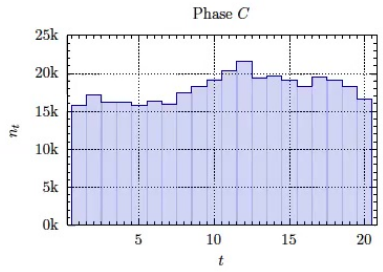


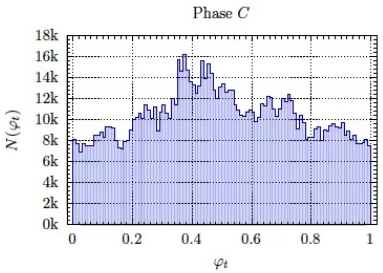

# De Sitter phase ($C_{dS}$)

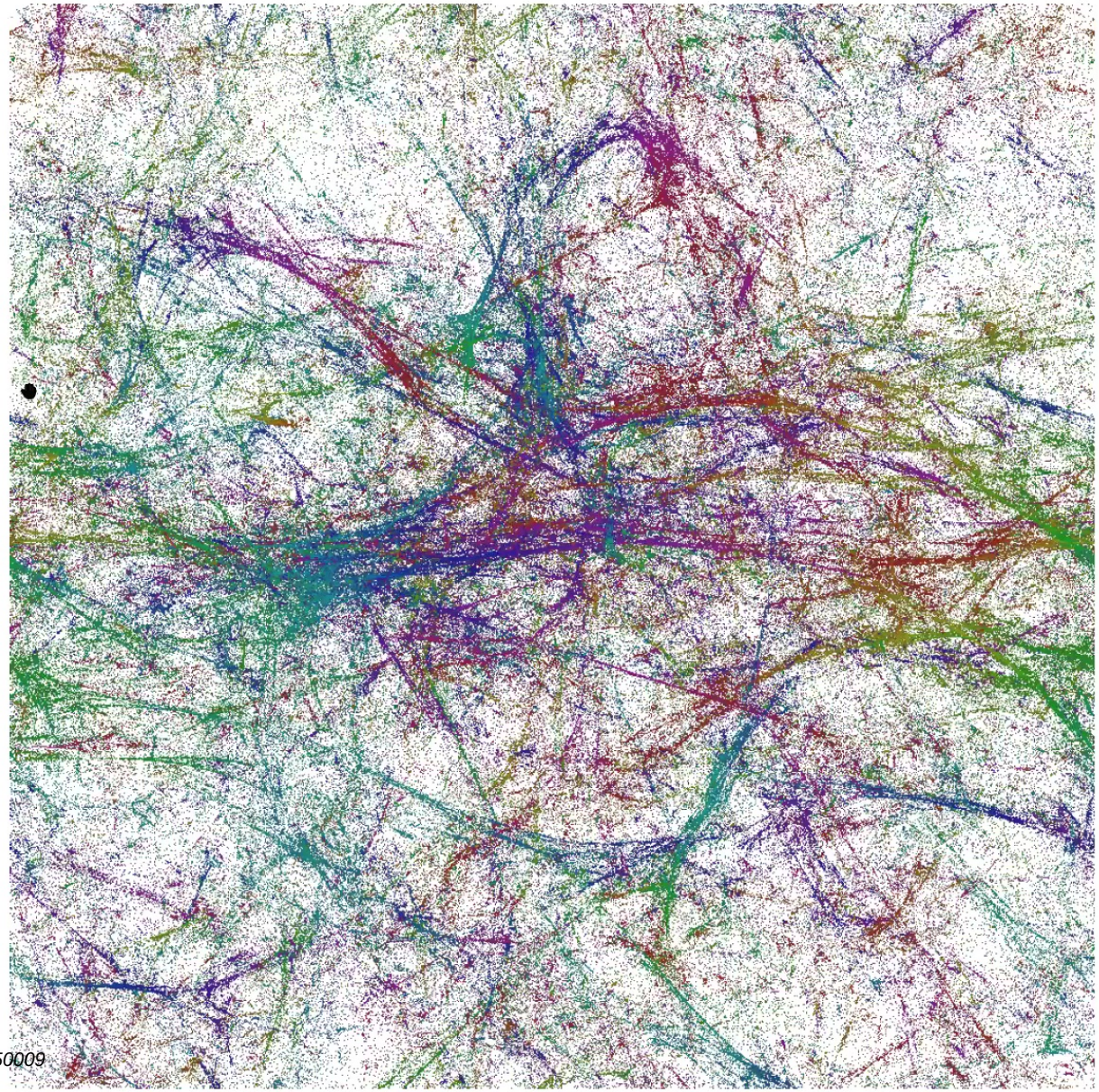

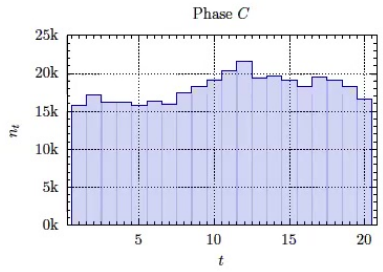


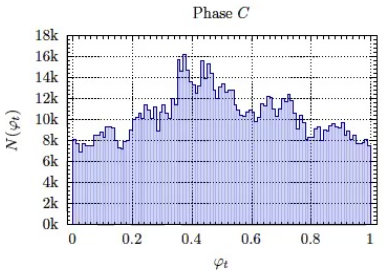

# Properties

- For a toroidal configuration, we can assign to each simplex $i$ a set of coordinates $(\varphi_i^x, \varphi_i^y, \varphi_i^z, \varphi_i^t)$ and plot the volume density distribution *(projection)*.
- The exact position of the boundary is irrelevant. After any *shift modulo-one* operation (boundary redefinition),

$$\varphi_i \to (\varphi_i + \text{const}) \mod 1,$$

  the points fit into a $[0,1]^4$ hypercube.
- The coordinates *preserve* the structure of the triangulation. Coordinates of each simplex are equal to the mean value of the coordinates of its neighbors.
- The coordinate $\varphi^t$ is not the same as the one coming from the original CDT foliation.

# De Sitter phase ($C_{dS}$)

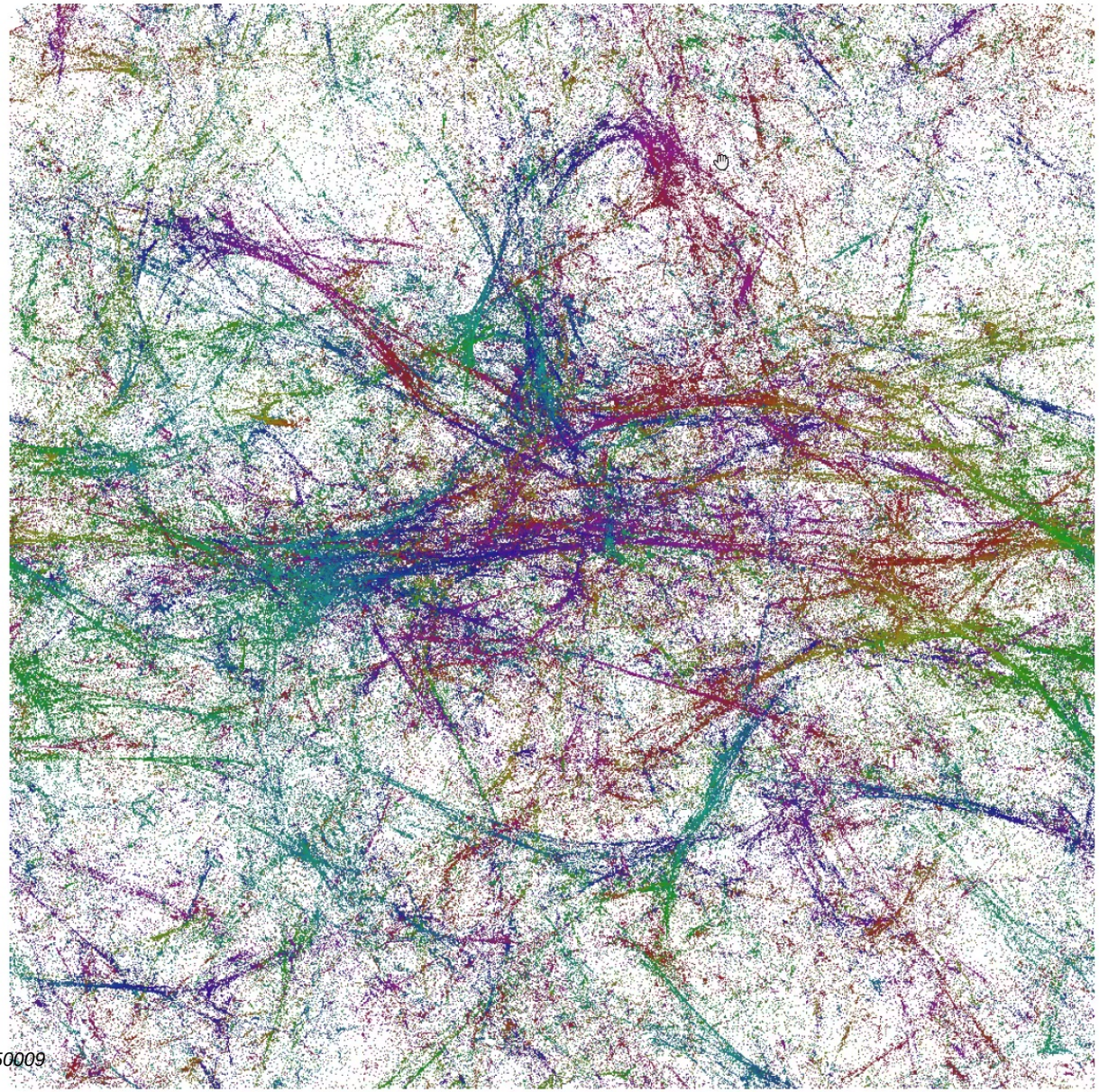

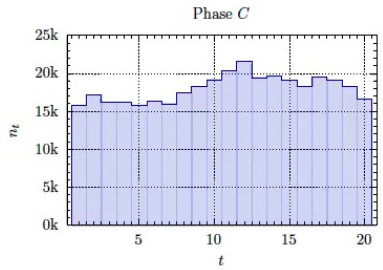


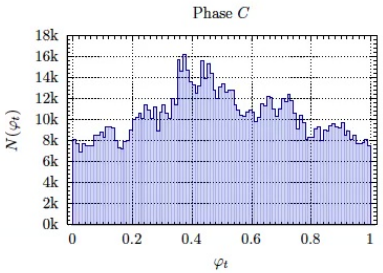

# Properties

- For a toroidal configuration, we can assign to each simplex $i$ a set of coordinates $(\varphi_i^x, \varphi_i^y, \varphi_i^z, \varphi_i^t)$ and plot the volume density distribution *(projection)*.
- The exact position of the boundary is irrelevant. After any *shift modulo-one* operation (boundary redefinition),

$$\varphi_i \to (\varphi_i + \text{const}) \mod 1,$$

  the points fit into a $[0,1]^4$ hypercube.
- The coordinates *preserve* the structure of the triangulation. Coordinates of each simplex are equal to the mean value of the coordinates of its neighbors.
- The coordinate $\varphi^t$ is not the same as the one coming from the original CDT foliation.

# Fractality

- We observe a remarkable pattern of voids and filaments, which qualitatively looks quite similar to the pictures of voids and filaments observed in our real Universe.
- The scalar field changes are smaller inside outgrowths. Outgrowths are visible as dense *clouds* of points *(large volume)*.

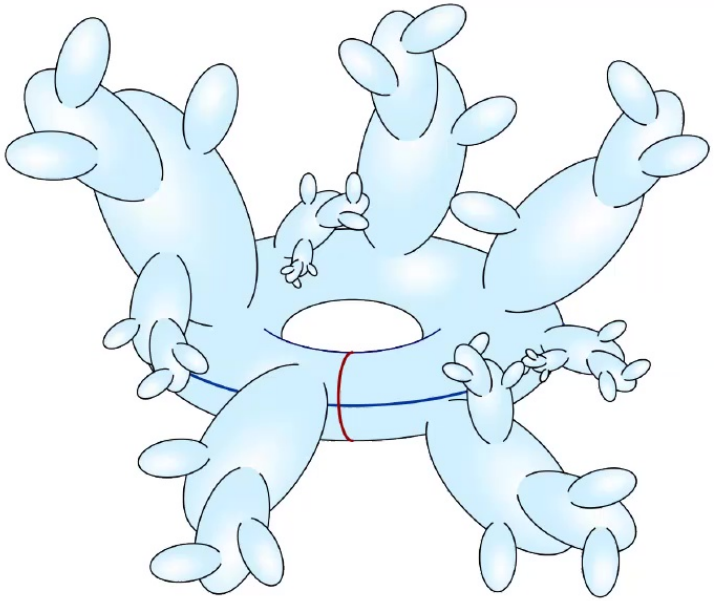

# Fractality

- We observe a remarkable pattern of voids and filaments, which qualitatively looks quite similar to the pictures of voids and filaments observed in our real Universe.
- The scalar field changes are smaller inside outgrowths. Outgrowths are visible as dense *clouds* of points *(large volume)*.

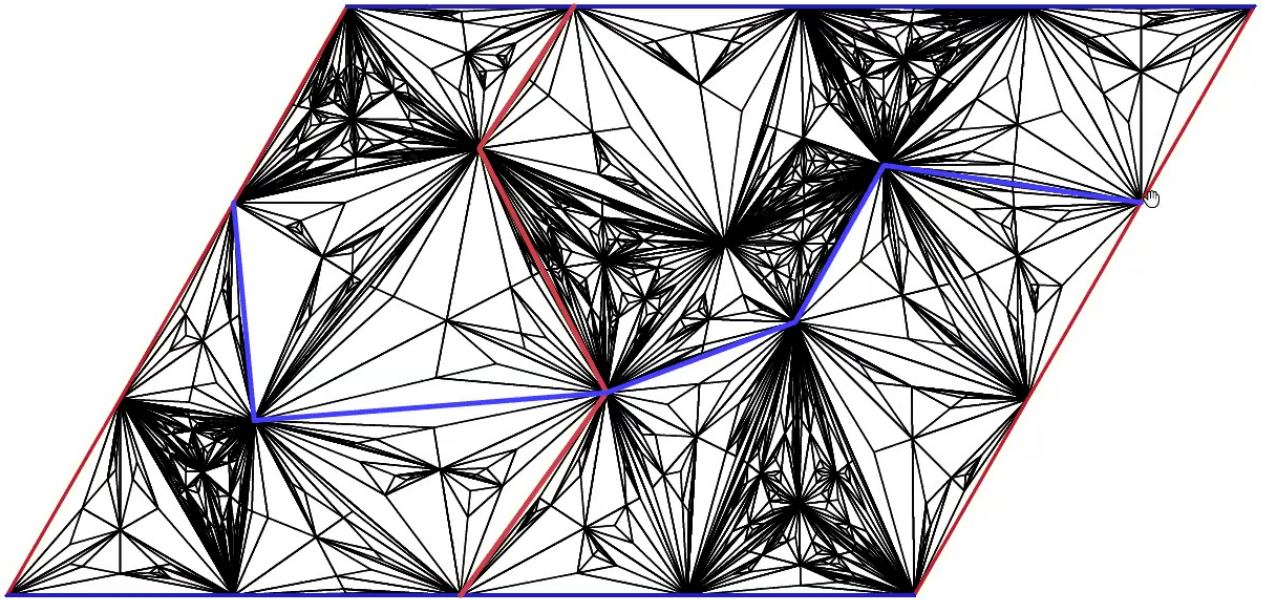

# De Sitter phase ($C_{dS}$)

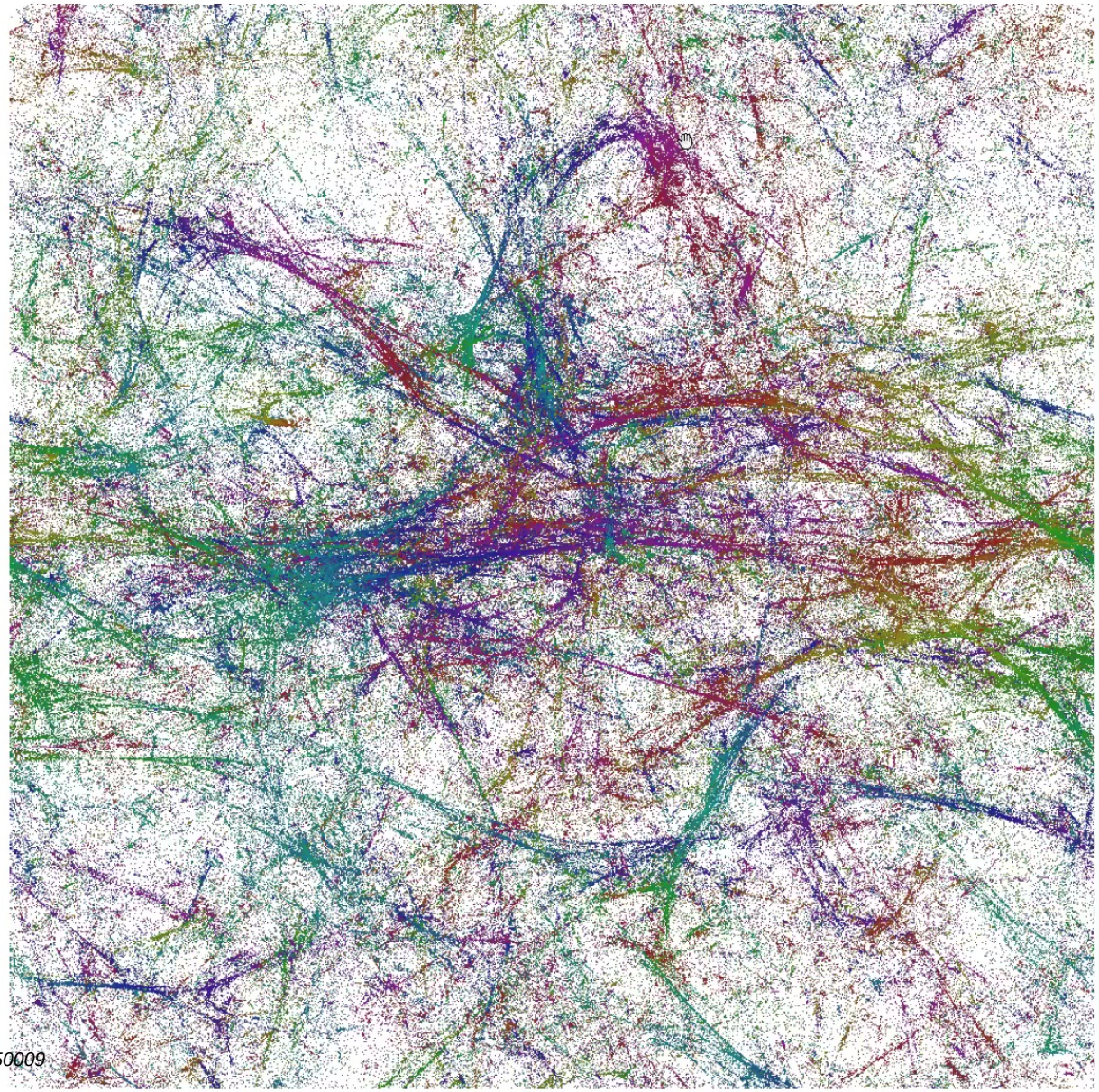

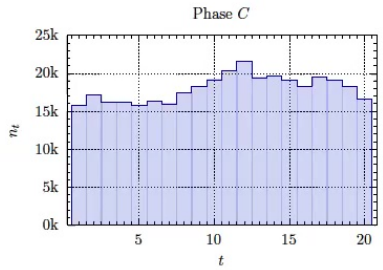


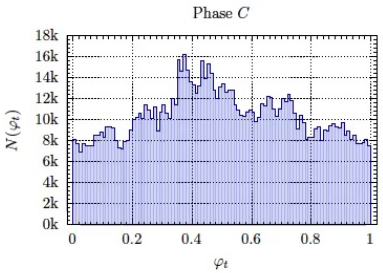

# Phase structure

- The Einstein-Hilbert action

$$S^{EH}[g] = -\frac{1}{G}\int \mathrm{d}t \int \mathrm{d}^D x \sqrt{g}(R - 2\Lambda)$$

- The Regge action

$$S^{R}[\mathcal{T}] = -K_0 N_0 + K_4 N_4 + \Delta(N_{41} - 6N_0)$$

- Parameters:

  $N_0$ number of vertices
  $N_4$ number of simplices
  $N_{41}$ number of simplices of type $\{4, 1\}$

- Three bare coupling constants:

  $K_0$ inverse gravitational constant, $K_0 \sim \frac{1}{G}$
  $K_4$ cosmological constant, $K_4 \sim \Lambda$ *(tuned)*
  $\Delta$ asymmetry factor, $\Delta \sim \frac{a_t}{a_s}$

- Rich phase structure: *A*, *B*, *Bifurcation*, ***C*** *(de Sitter)*.

# Phase structure

Tuned cosmological constant

$$S[\mathcal{T}] = -K_0 N_0 + K_4 N_4 + \Delta(N_{14} - 6N_0)$$

Two coupling constants

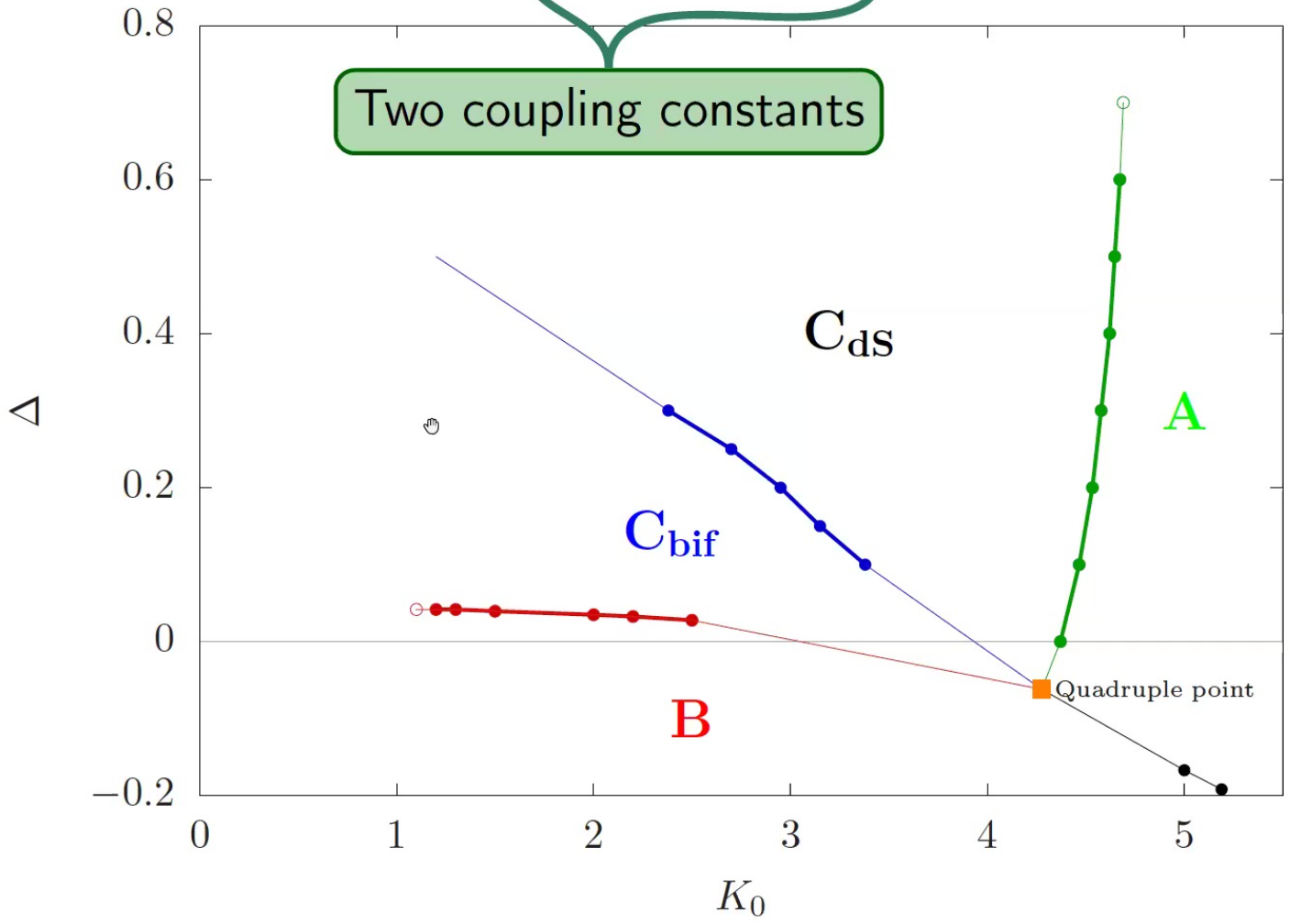

# Phase $A$

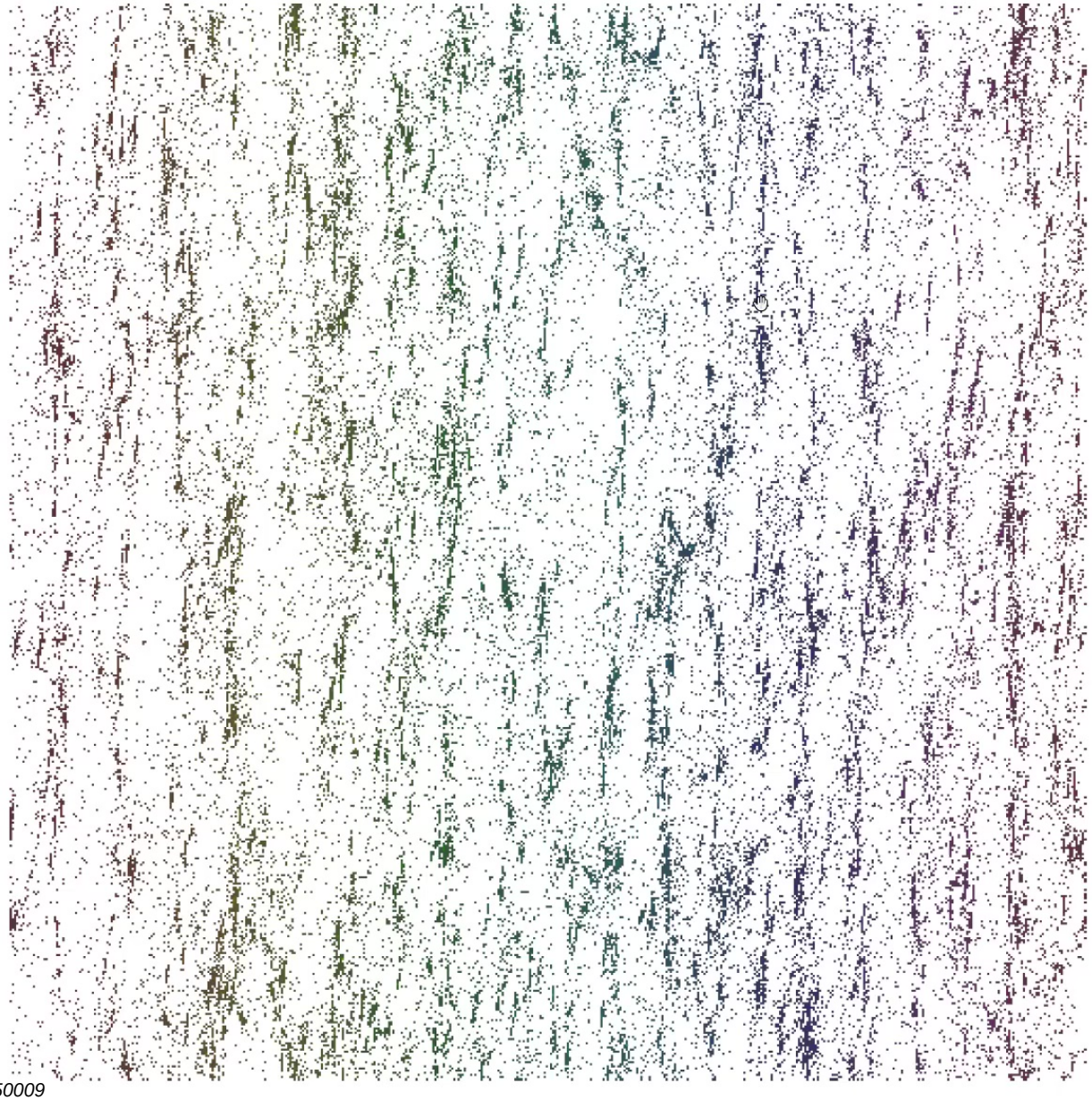

$\varphi_t - \varphi_x$

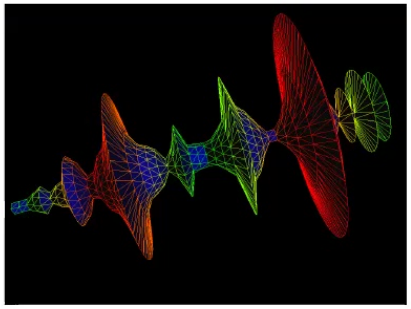

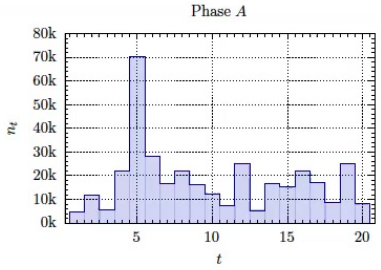


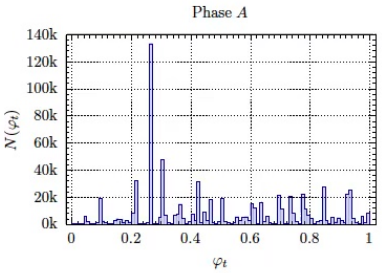

# Bifurcation phase ($C_b$)

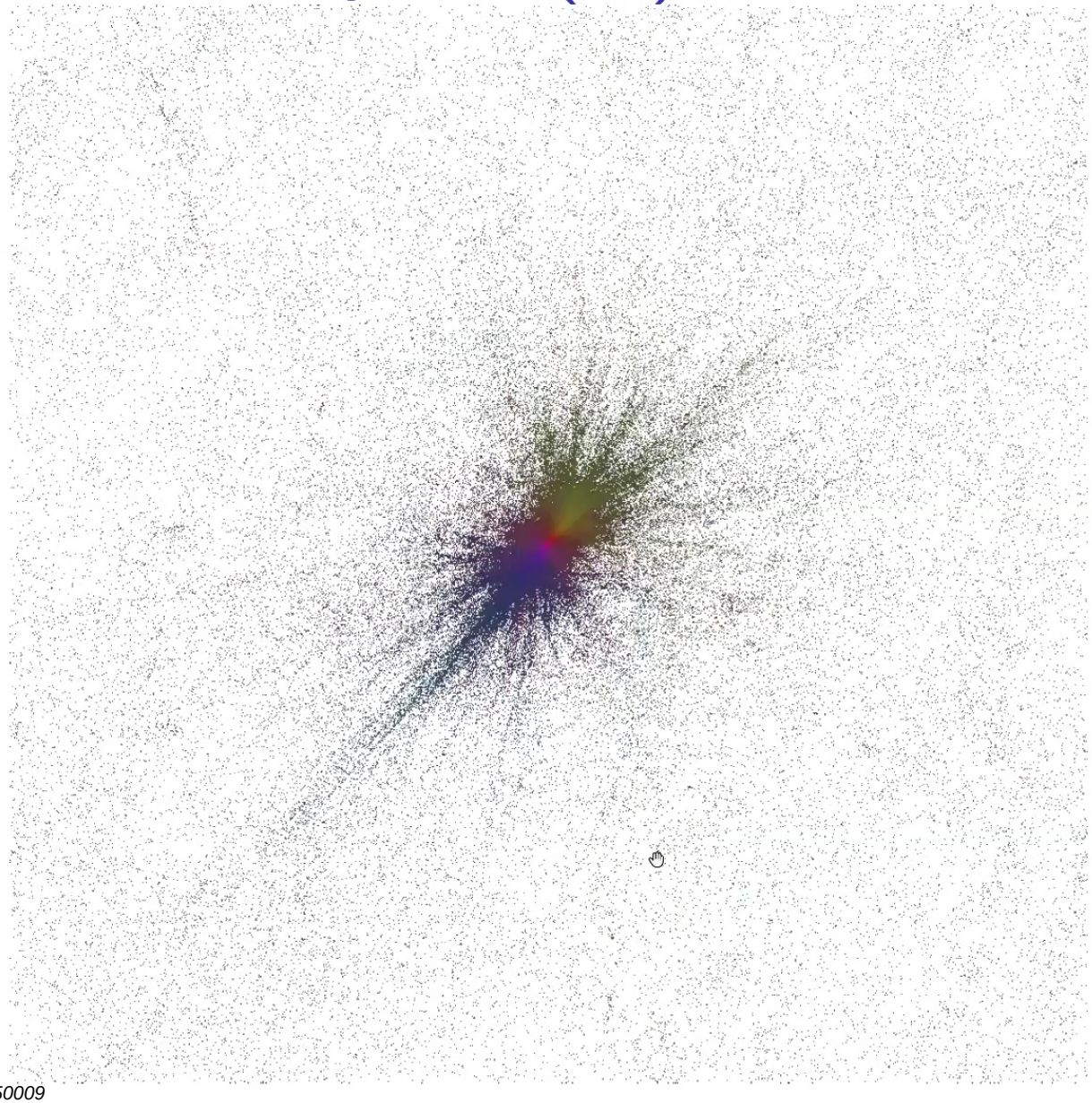

$\varphi_x - \varphi_y$

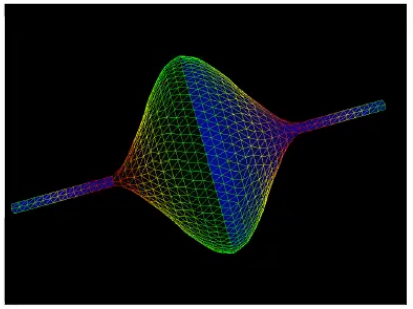

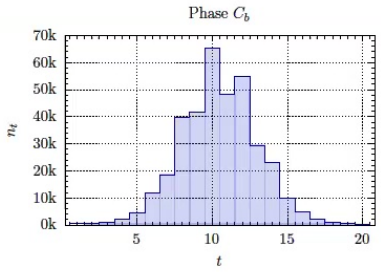


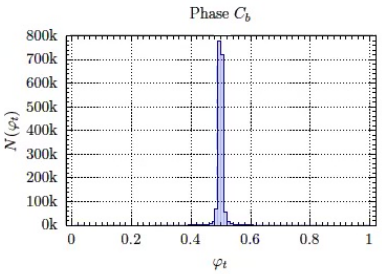

# Phase $B$

$\varphi_t - \varphi_x$

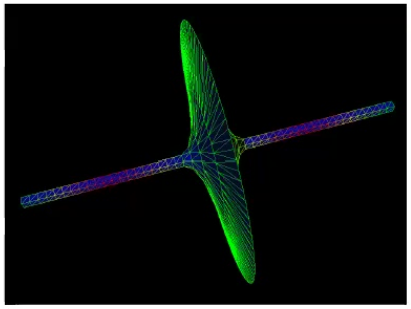

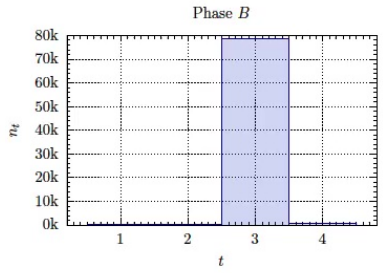


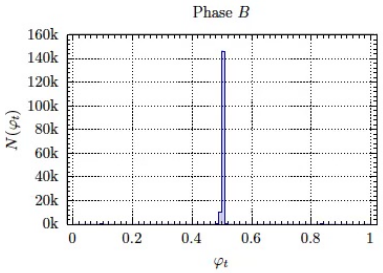

# Phase $B$

$\varphi_x - \varphi_y$

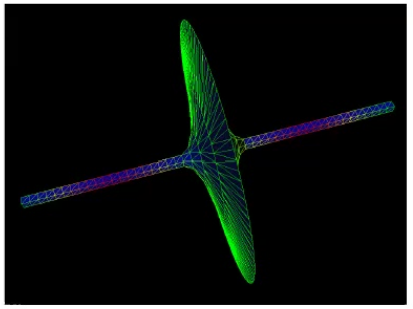

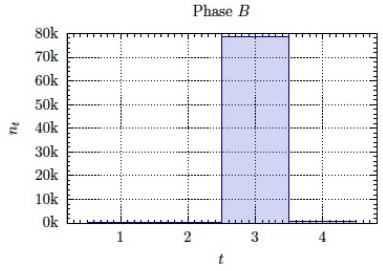


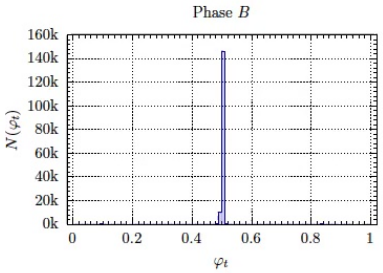

# Dynamical scalar fields

- Thus far, the scalar field was only used to introduce coordinates on an existing triangulation and had no dynamical impact.
- *What effect do dynamical fields have on the underlying (quantum) geometric degrees of freedom?*
- The continuous Euclidean action for a massless scalar field:

$$S[g,\varphi] = \frac{1}{2}\int \mathrm{d}^4x\,\sqrt{g(x)}\,\partial^\mu\varphi(x)\partial_\mu\varphi(x), \quad \varphi(x)\in S^1(\delta)$$

- The discrete counterpart of the matter action decomposes into the quantum and the classical parts:

$$\begin{aligned} S[\mathcal{T},\varphi=\bar{\varphi}+\eta] &= \sum_{i\leftrightarrow j}(\varphi_i-\varphi_j-\delta \mathrm{B}_{ij})^2 \\ &= \eta^\top \mathrm{L}\eta + \delta^2\tilde{S}^{\mathrm{clas}}[\mathcal{T}] \\ \tilde{S}^{\mathrm{clas}}[\mathcal{T}] &= \tilde{\varphi}^\top \mathrm{L}\tilde{\varphi} - 2b^\top\tilde{\varphi} + \|\mathrm{B}\|^2, \quad L\tilde{\varphi}=b \end{aligned}$$

# Jump in time direction

One scalar field with periodic boundary conditions and a jump of size $\delta$ in time direction.

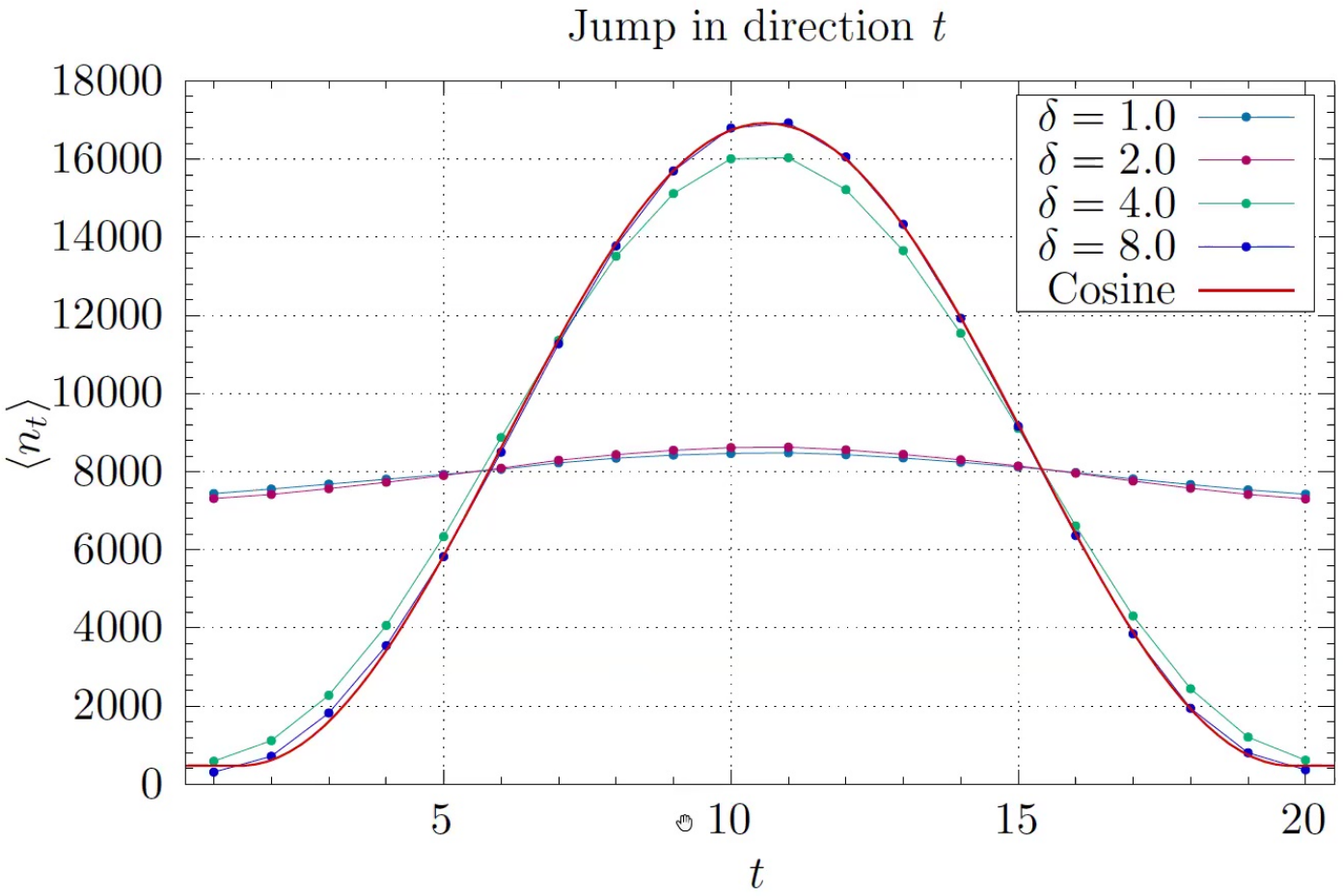

# Minisuperspace model with scalar field

## Minisuperspace action

$$S[v,\varphi] = \int \mathrm{d}^4x\,\sqrt{g}\left(\#R - \Lambda + (\partial\varphi)^2\right), v \propto a^3(t)$$

## Constraints

$$V = \int \mathrm{d}t\, v, \quad \delta = \int \mathrm{d}t\,\dot{\varphi} = \varphi\left(\frac{T}{2}\right) - \varphi\left(-\frac{T}{2}\right), \quad v(t) \geq \varepsilon$$

## Constant solution for $\delta \leq 2\pi$

$$v(t) = \frac{V}{T}, \qquad \dot{\varphi}(t) = \frac{\delta}{T}, \qquad S = \frac{V}{T^2}\cdot\delta^2$$

## Cosine solution for $\delta \geq 2\pi$

$$v(t) = \begin{cases} c\cdot\cos\left(\frac{2\pi}{\tau}t\right) + c + \varepsilon & |t| \leq \frac{\tau}{2} \\ \varepsilon & \frac{\tau}{2} \leq |t| \leq \frac{T}{2} \end{cases}, \quad \dot{\varphi}(t) = \frac{\beta}{v(t)}$$

# Minisuperspace model with scalar field

## Classical solutions

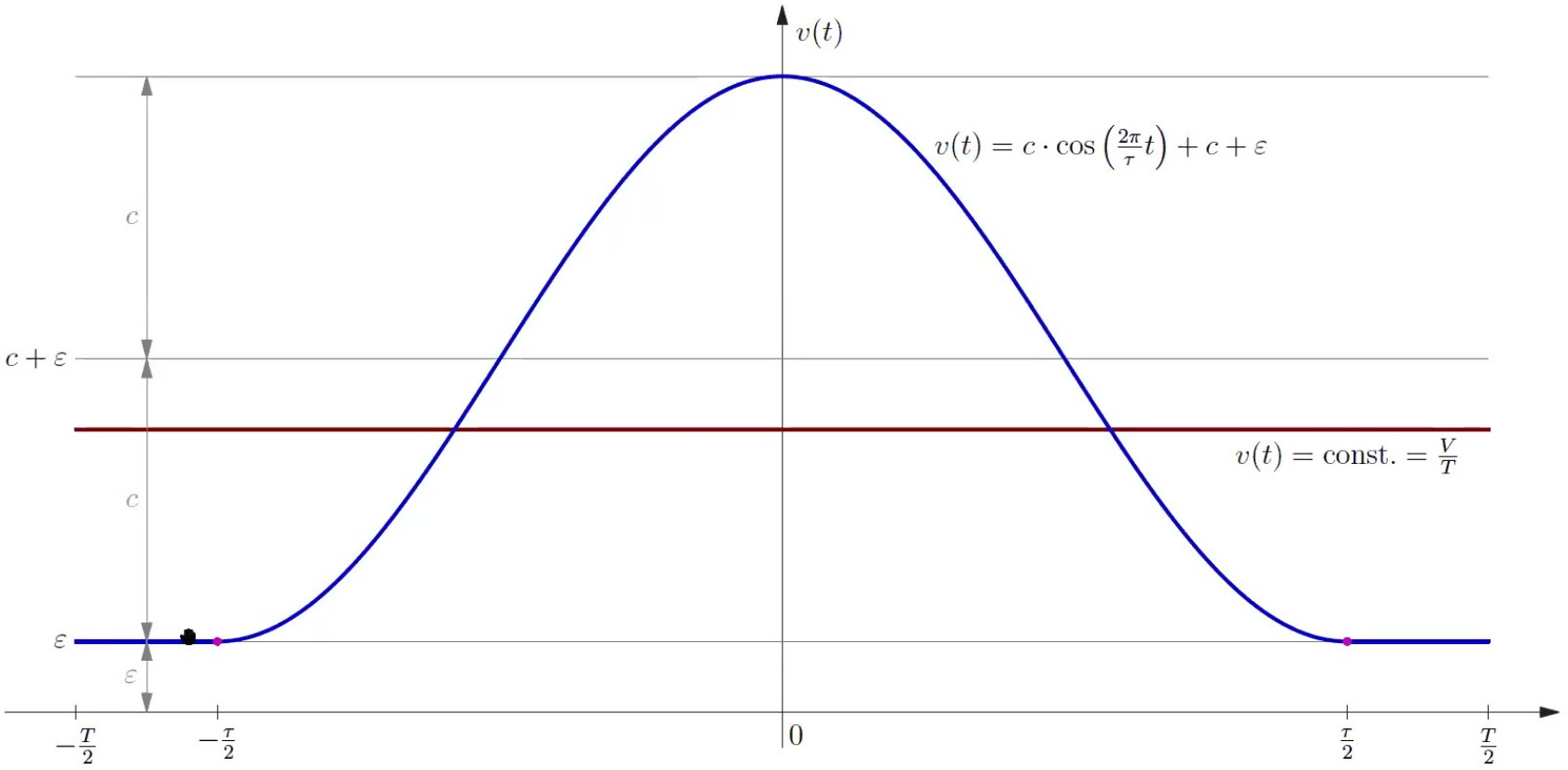


Phase transition at $\delta = \frac{2\pi}{\sqrt{G}}$

# Minisuperspace model with scalar field

## Minisuperspace action

$$S[v,\varphi] = \int_{-T/2}^{T/2} \mathrm{d}t\, \frac{\dot{v}^2}{v} + v\dot{\varphi}^2, \qquad v = v(t) \propto a^3(t),\ \varphi = \varphi(t)$$

## Constraints

$$V = \int \mathrm{d}t\, v, \quad \delta = \int \mathrm{d}t\, \dot{\varphi} = \varphi\left(\frac{T}{2}\right) - \varphi\left(-\frac{T}{2}\right), \quad v(t) \geq \varepsilon$$

## Constant solution for $\delta \leq 2\pi$

$$v(t) = \frac{V}{T}, \qquad \dot{\varphi}(t) = \frac{\delta}{T}, \qquad S = \frac{V}{T^2} \cdot \delta^2$$

## Cosine solution for $\delta \geq 2\pi$

$$v(t) = \begin{cases} c \cdot \cos\left(\frac{2\pi}{\tau} t\right) + c + \varepsilon & |t| \leq \frac{\tau}{2} \\ \varepsilon & \frac{\tau}{2} \leq |t| \leq \frac{T}{2} \end{cases}, \quad \dot{\varphi}(t) = \frac{\beta}{v(t)}$$

# Minisuperspace model with scalar field

## Classical solutions

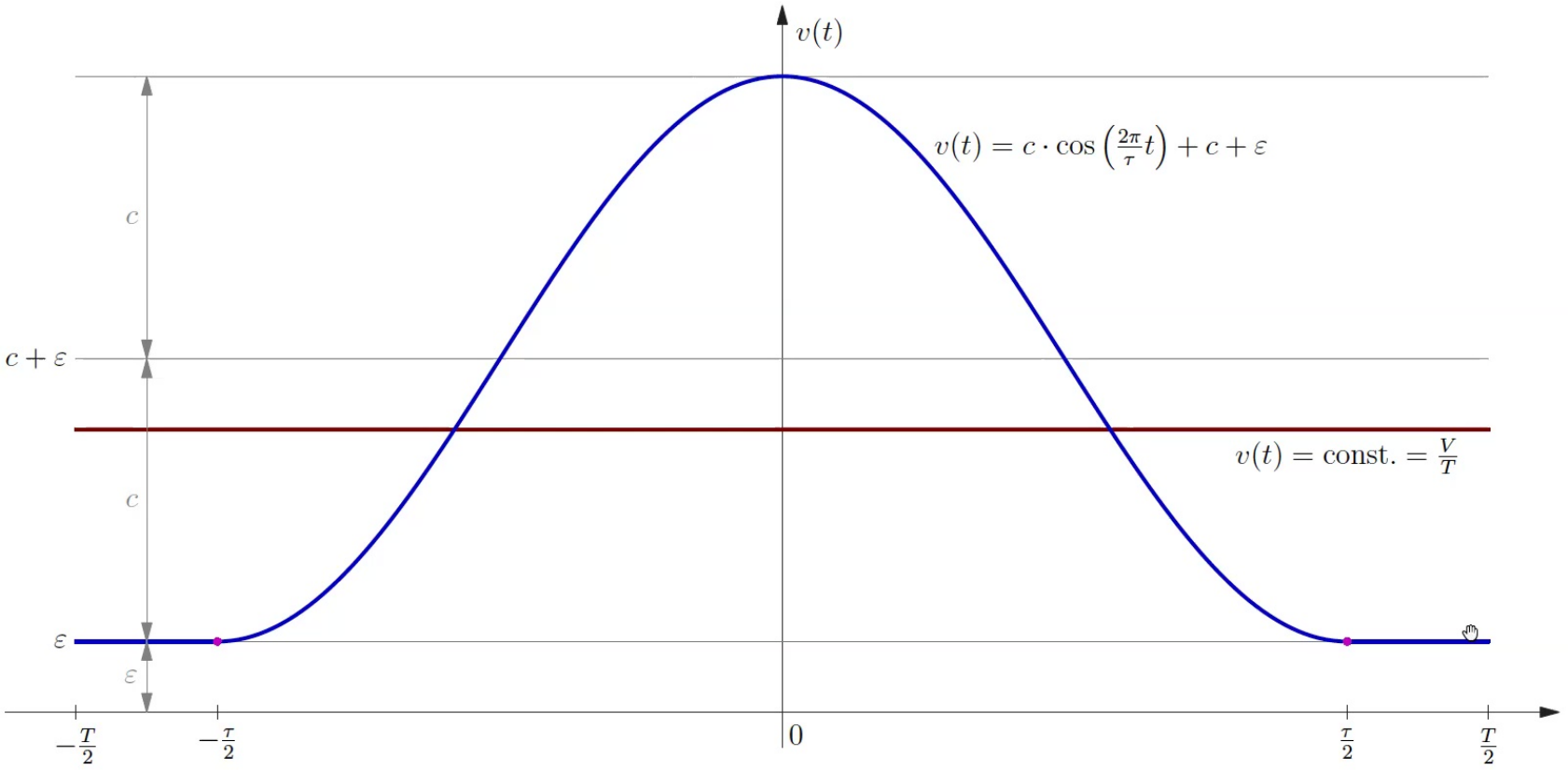


Phase transition at $\delta = \frac{2\pi}{\sqrt{G}}$

# Jump in time direction

One scalar field with periodic boundary conditions and a jump of size $\delta$ in time direction.

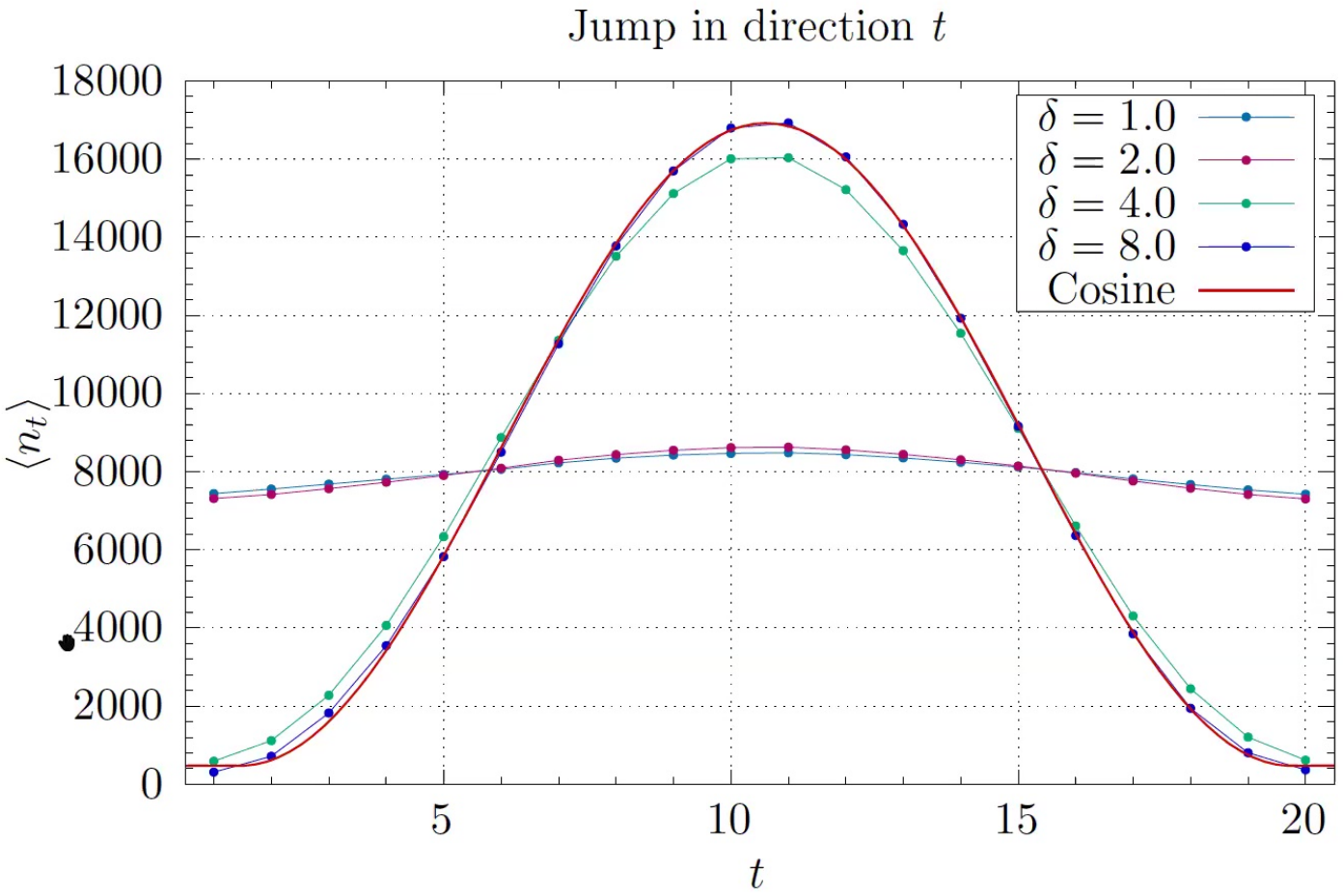

# Minisuperspace model with scalar field

## Classical action

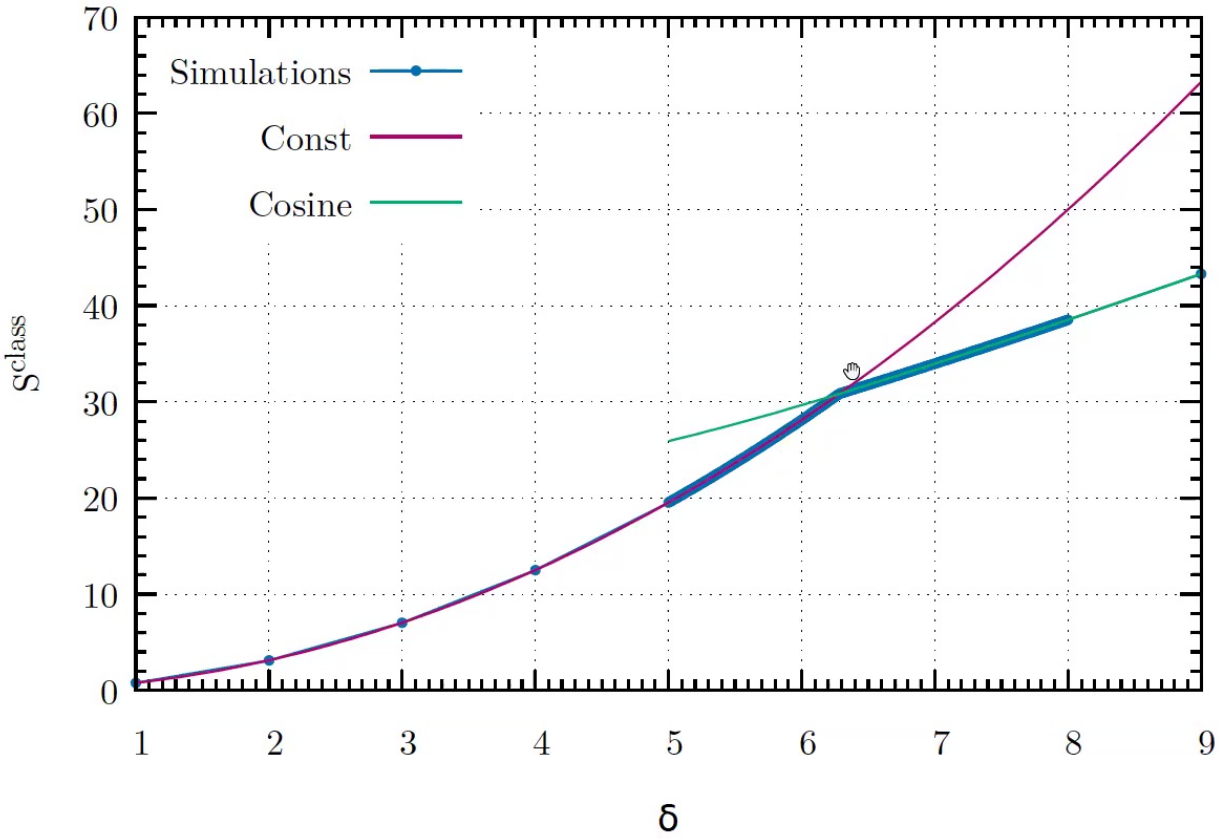


Phase transition at $\delta = \frac{2\pi}{\sqrt{G}}$

# Minisuperspace model with scalar field

## Classical solutions

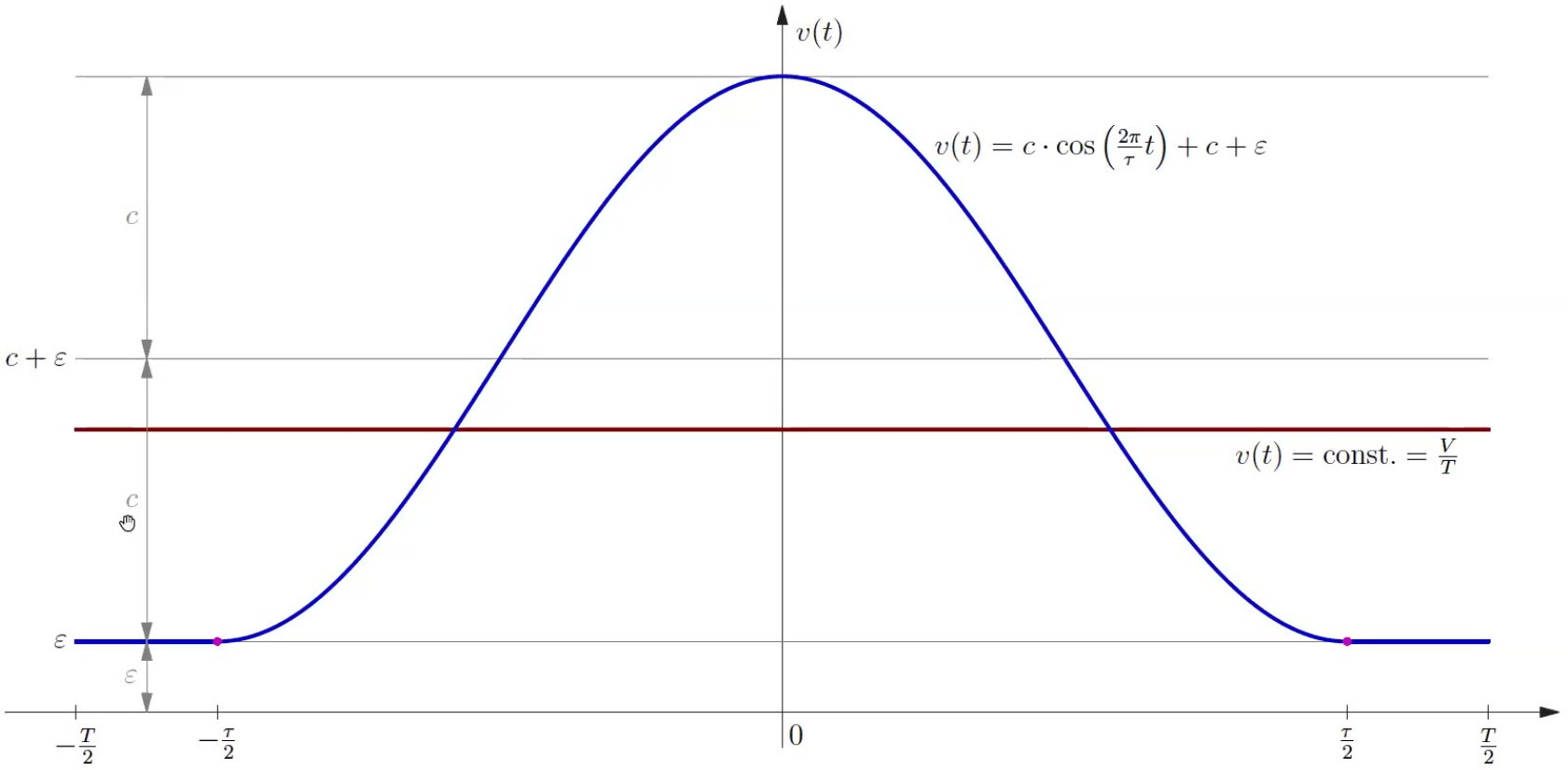


Phase transition at $\delta = \frac{2\pi}{\sqrt{G}}$

# Jump in time direction

One scalar field with periodic boundary conditions and a jump of size $\delta$ in time direction.

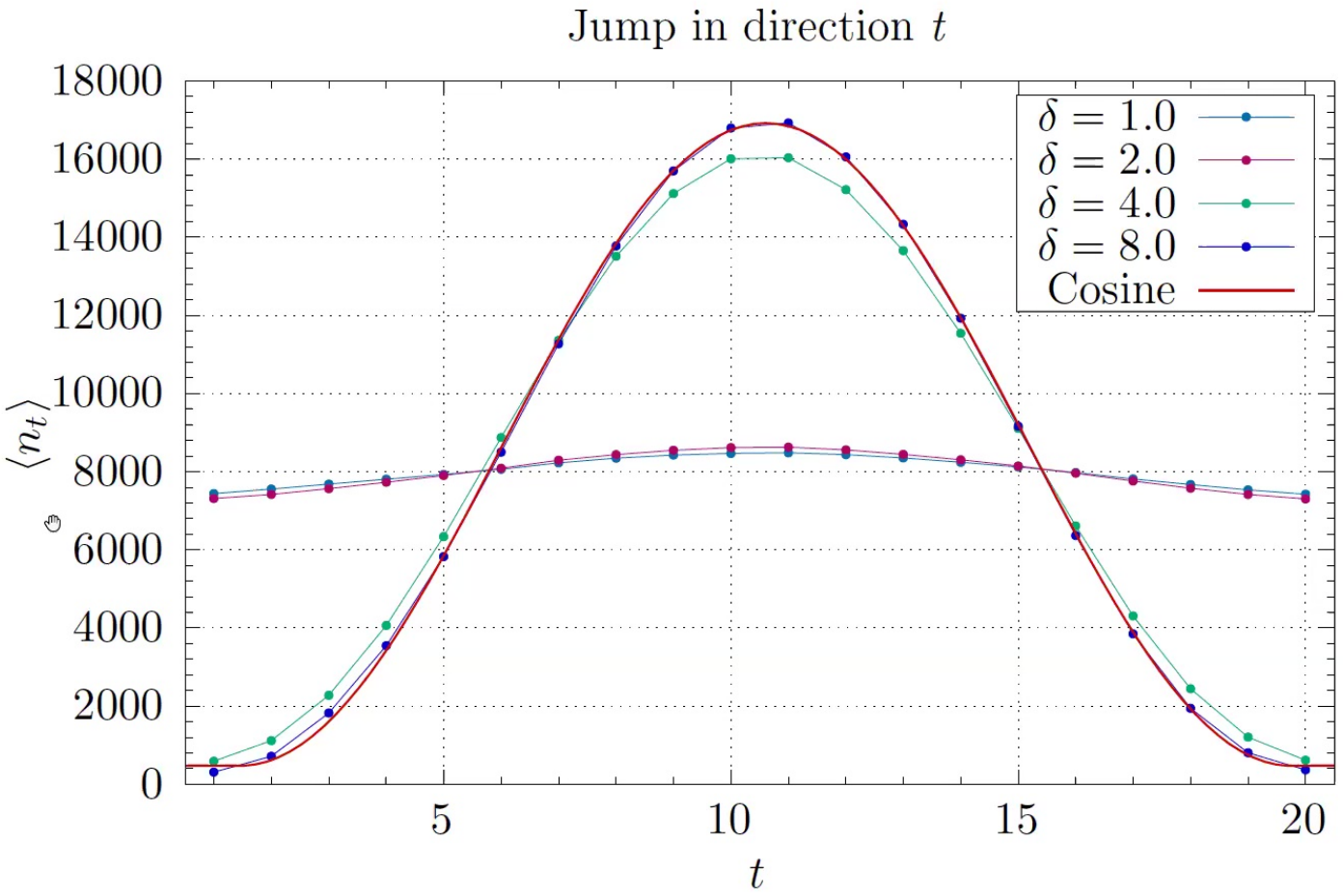

# Jumps in spatial directions

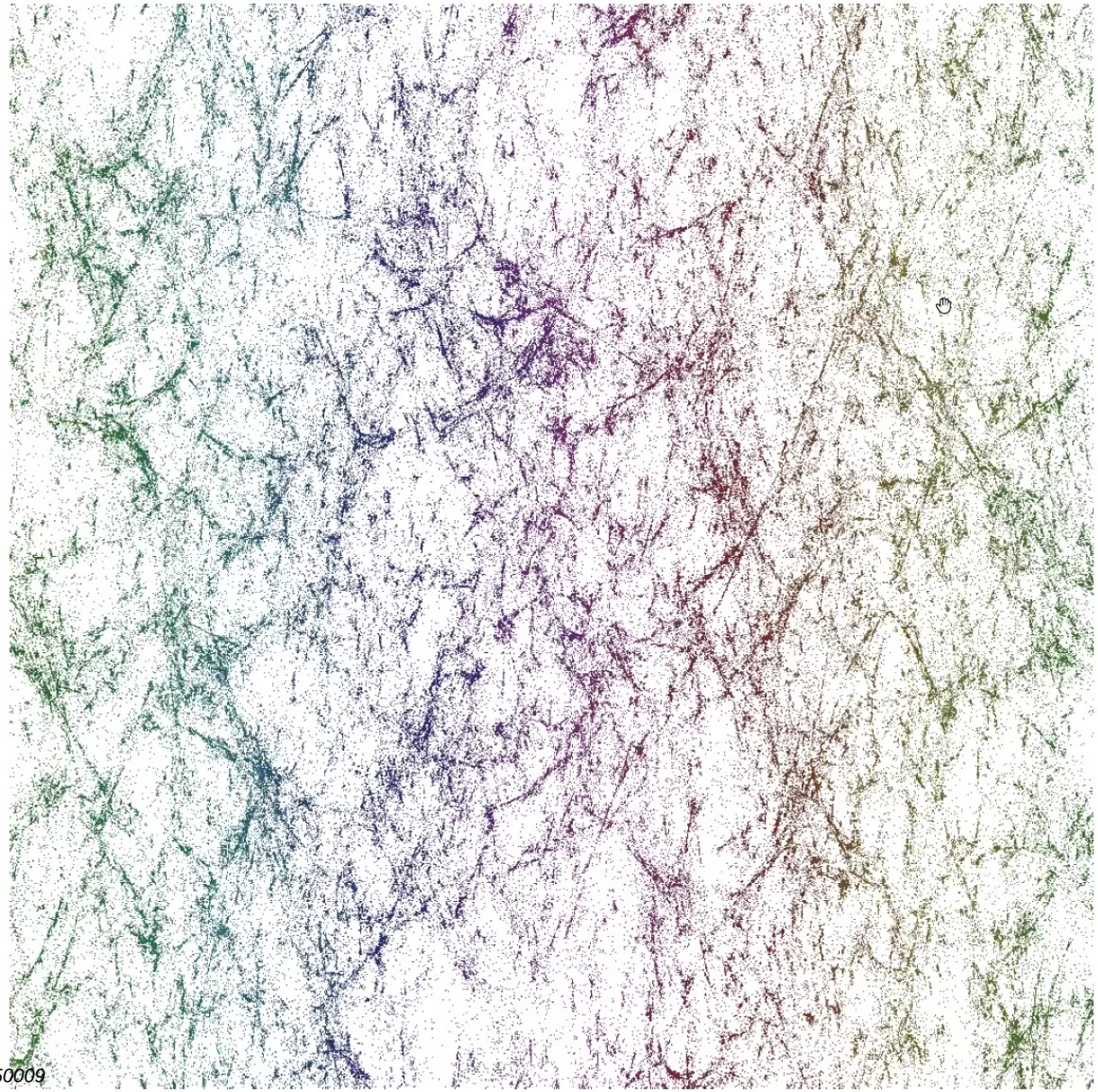

Three fields $\varphi^x, \varphi^y, \varphi^z$ with a jump $\delta = 1.0$. Projection on $\varphi^t - \varphi^x$.

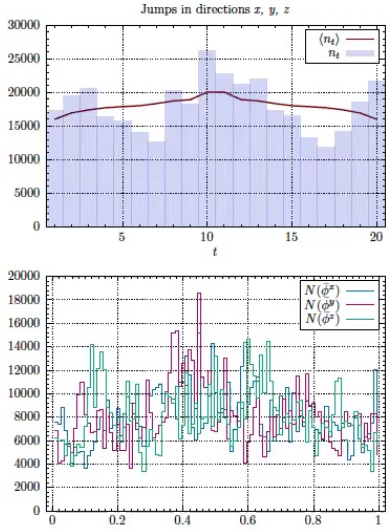

# Jumps in spatial directions

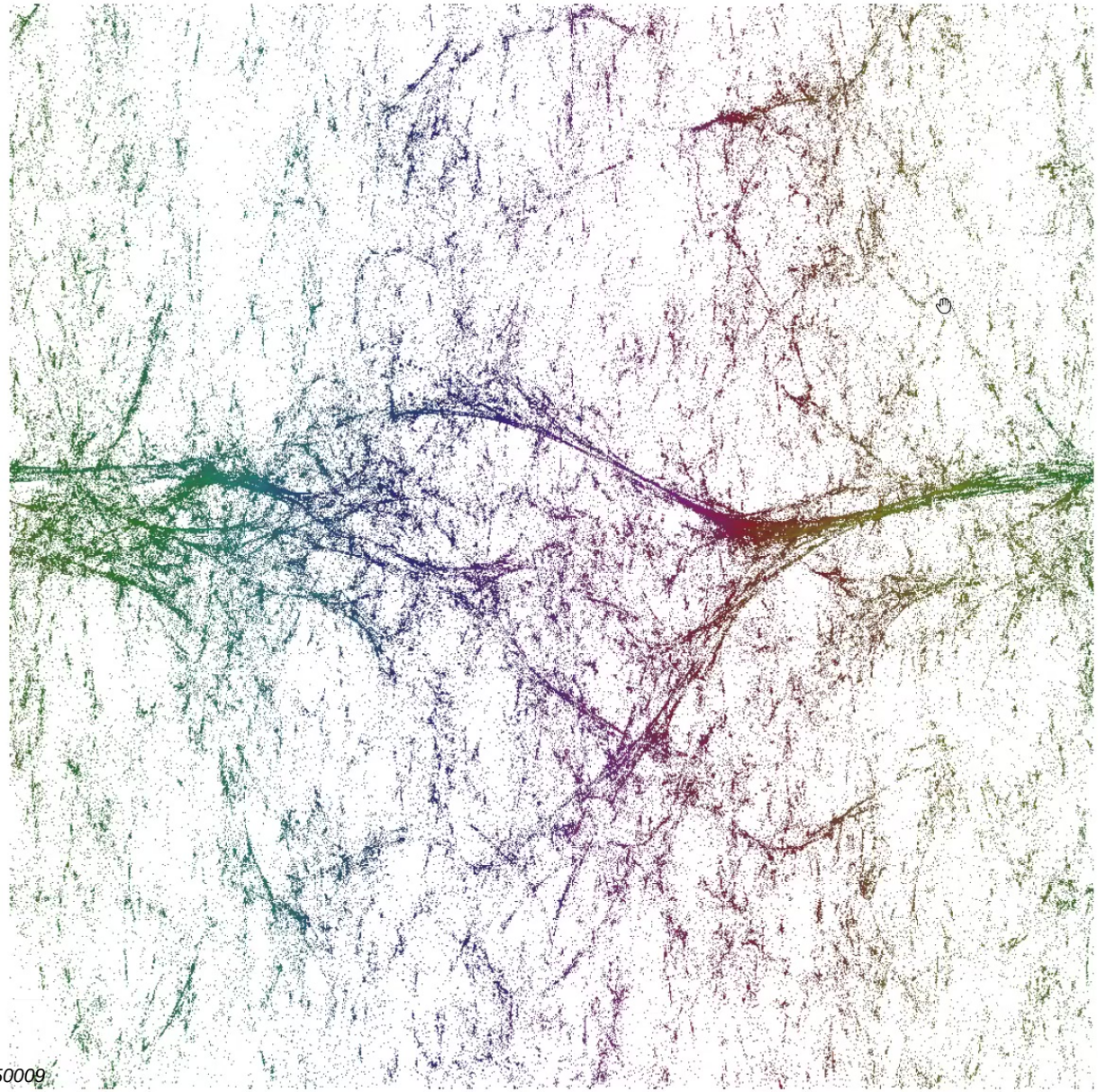

Three fields $\varphi^x, \varphi^y, \varphi^z$ with a jump $\delta = 2.5$. Projection on $\varphi^t - \varphi^x$.

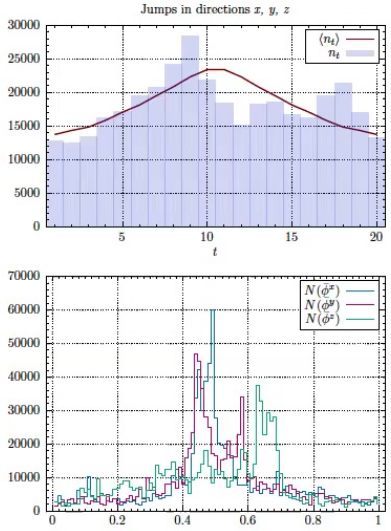

# Minisuperspace model with scalar field

## Classical action

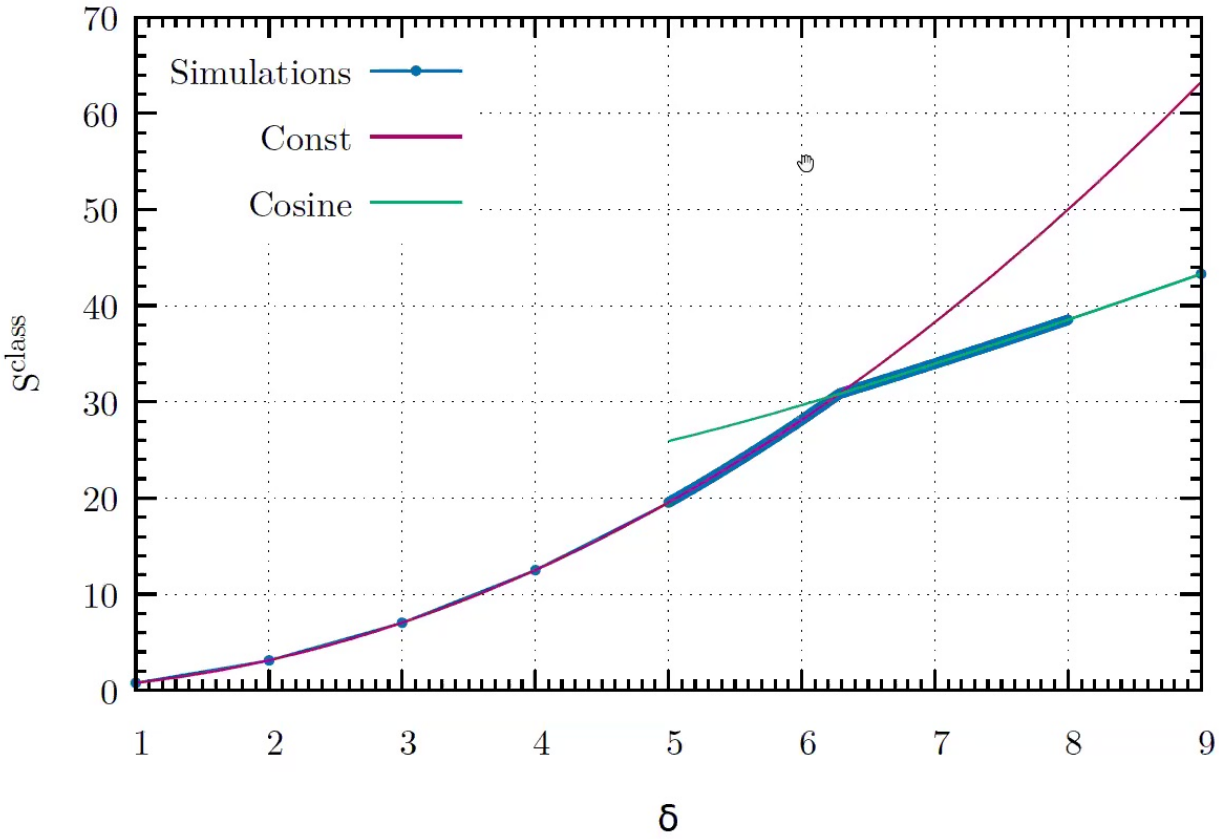


Phase transition at $\delta = \frac{2\pi}{\sqrt{G}}$

# Minisuperspace model with scalar field

## Classical solutions

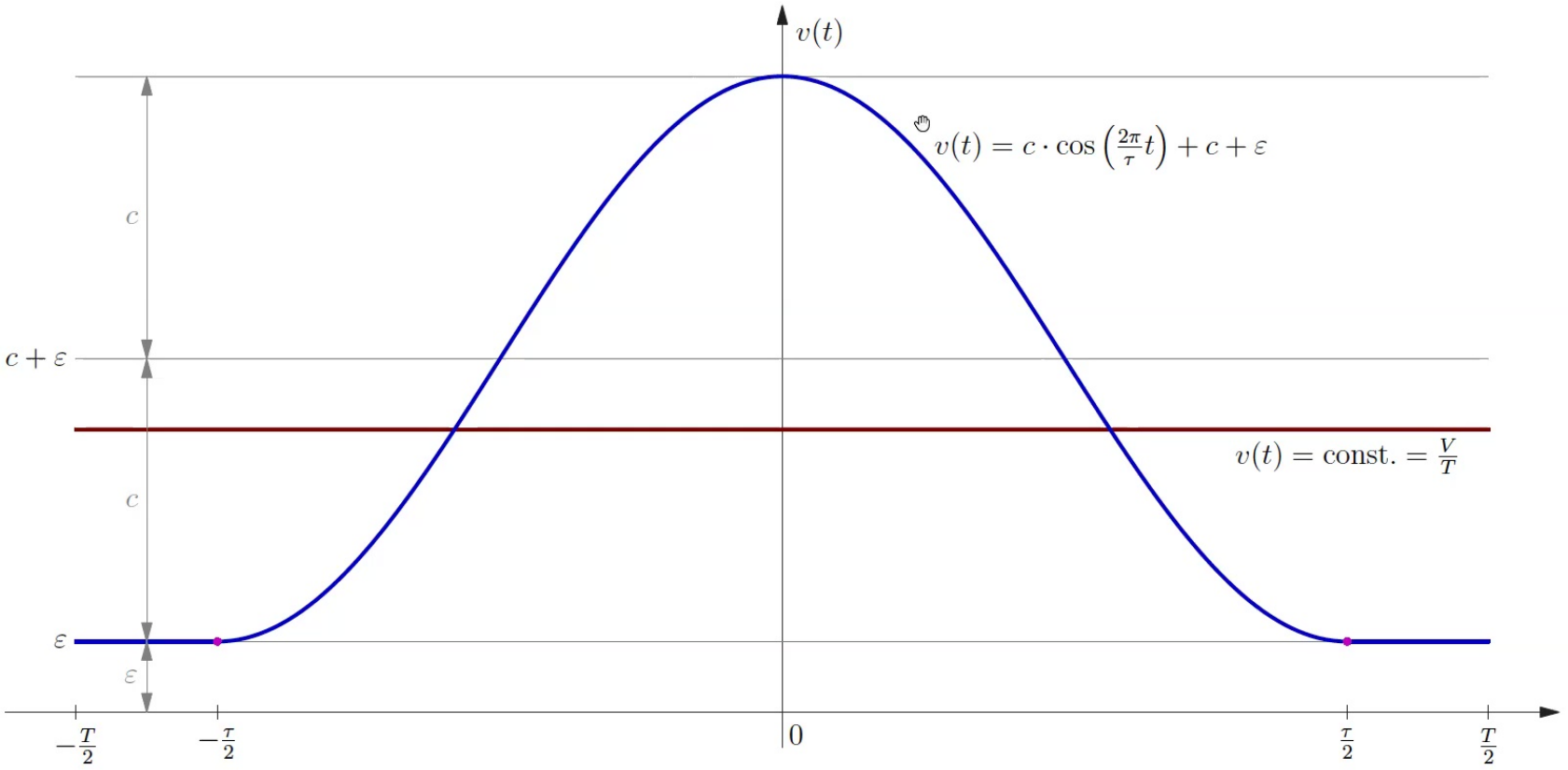


Phase transition at $\delta = \frac{2\pi}{\sqrt{G}}$

# Jumps in spatial directions

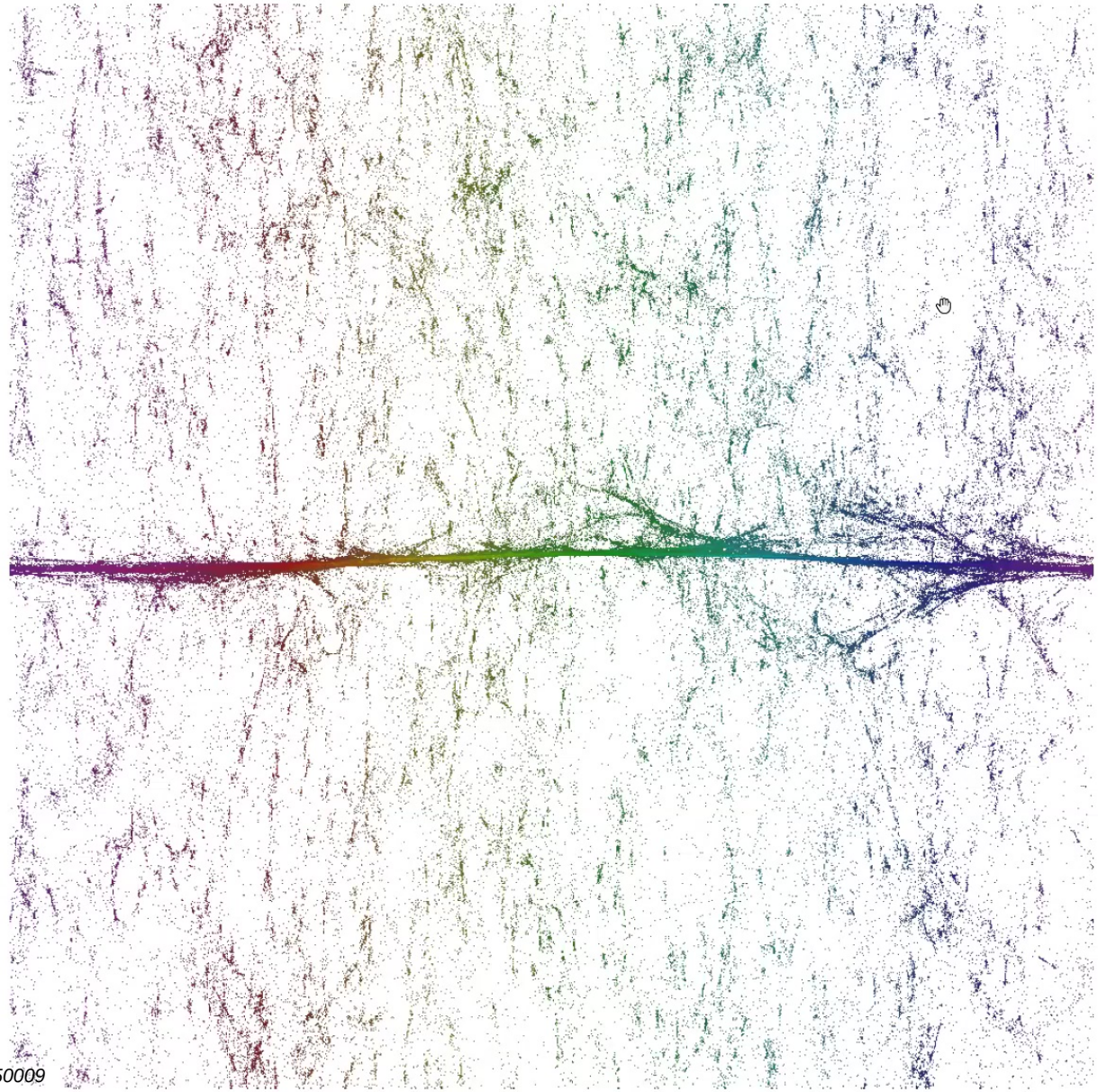

Three fields $\varphi^x, \varphi^y, \varphi^z$ with a jump $\delta = 4.0$. Projection on $\varphi^t - \varphi^x$.

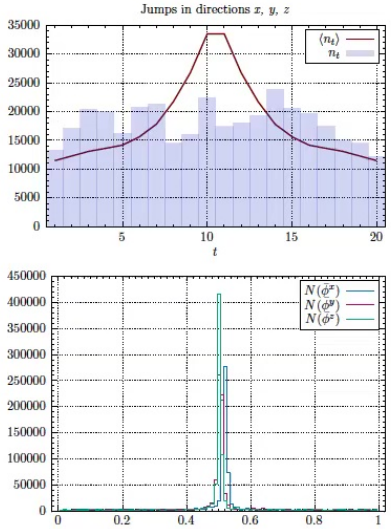

# Jumps in spatial directions

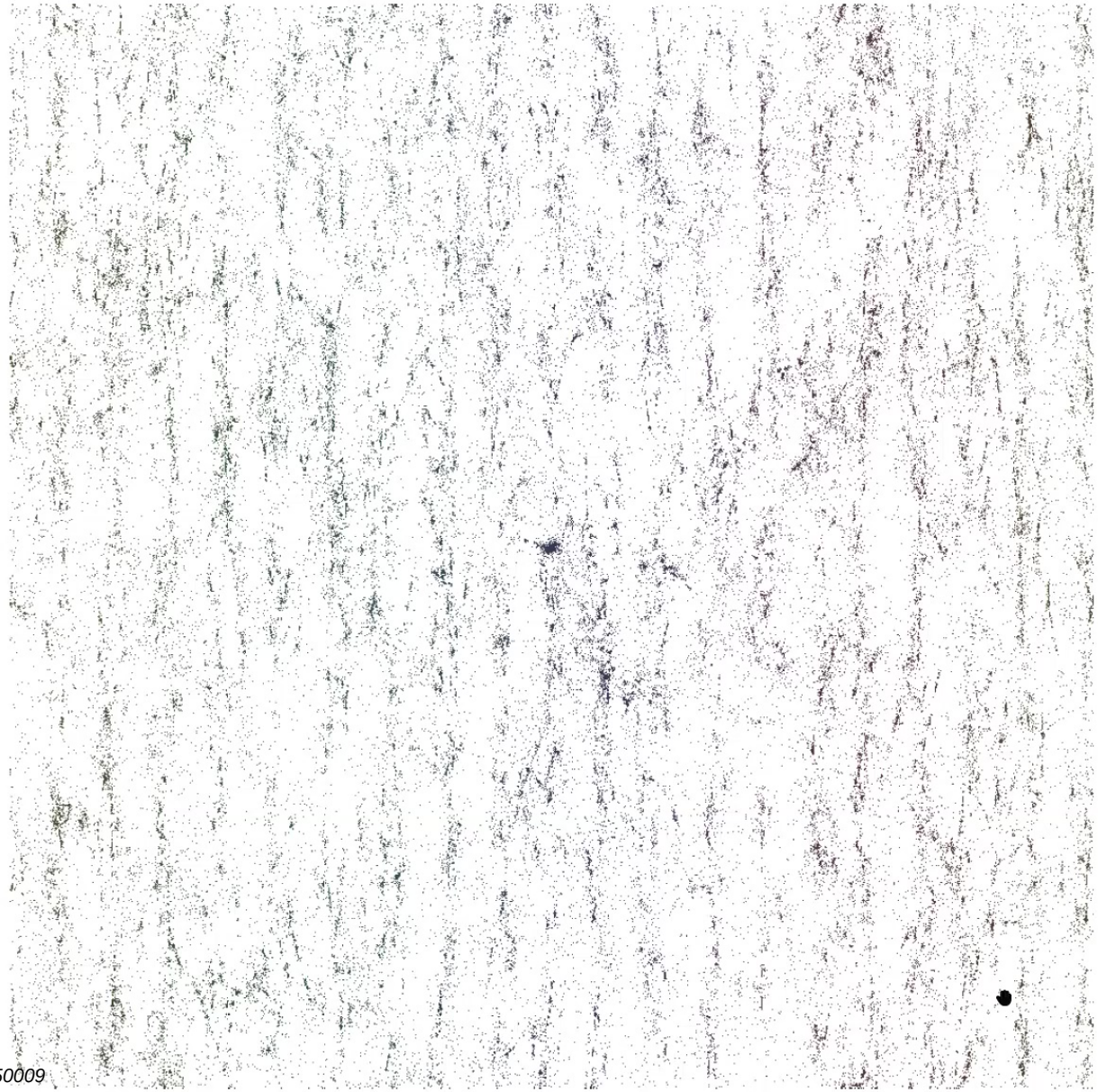

Three fields $\varphi^x, \varphi^y, \varphi^z$ with a jump $\delta = 10.0$. Projection on $\varphi^t - \varphi^x$.

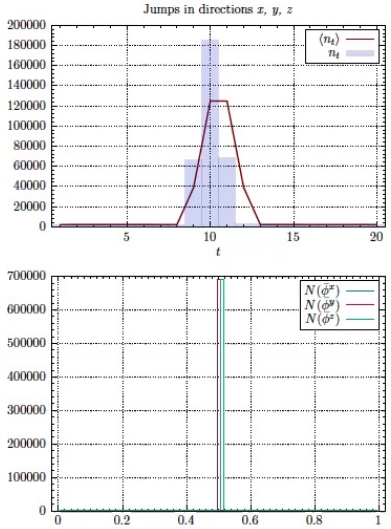

# Jumps in spatial directions

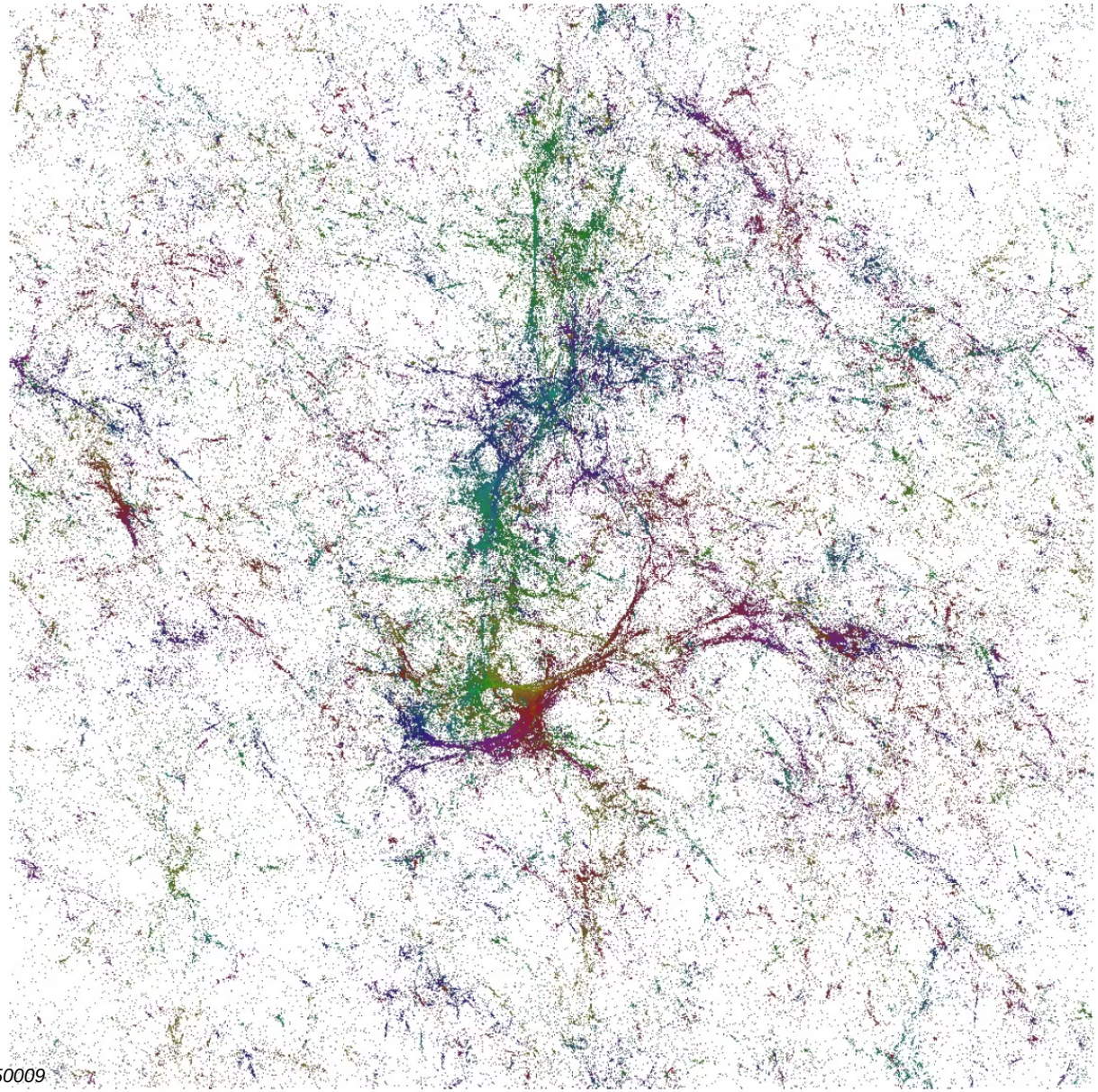

Three fields $\varphi^x, \varphi^y, \varphi^z$ with a jump $\delta = 2.5$. Projection on $\varphi^x - \varphi^y$.

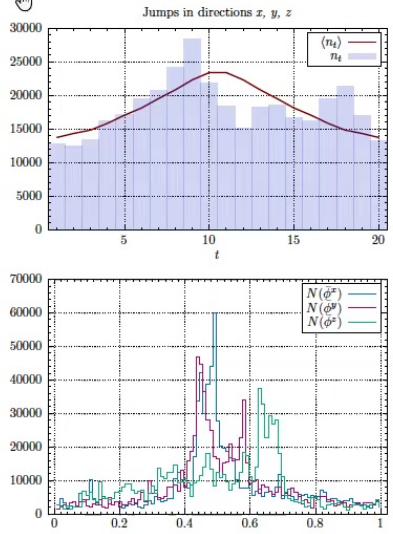

# Jumps in directions $x$, $y$, $z$ with $\delta = 7.0$

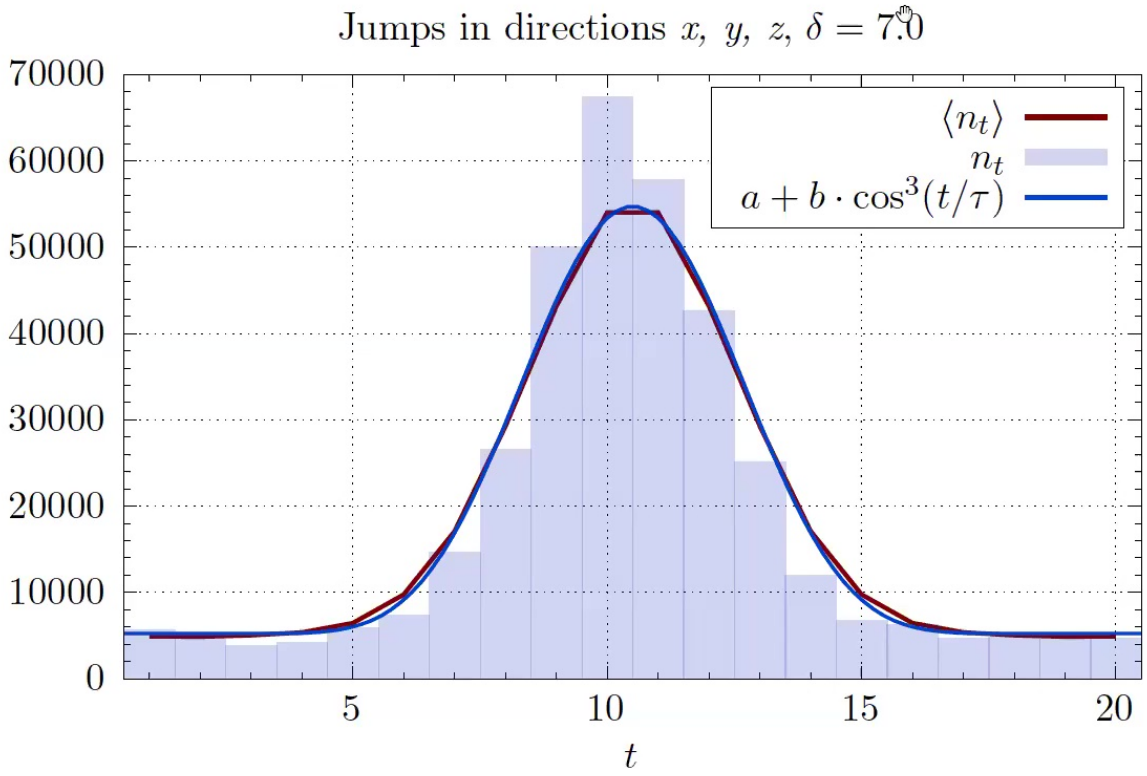

# Topology change

A scalar field with a strong enough jump ($\delta$) in a spatial direction introduces a *pinching* ($\varepsilon$), which results in an *effective* **change of spatial topology**.

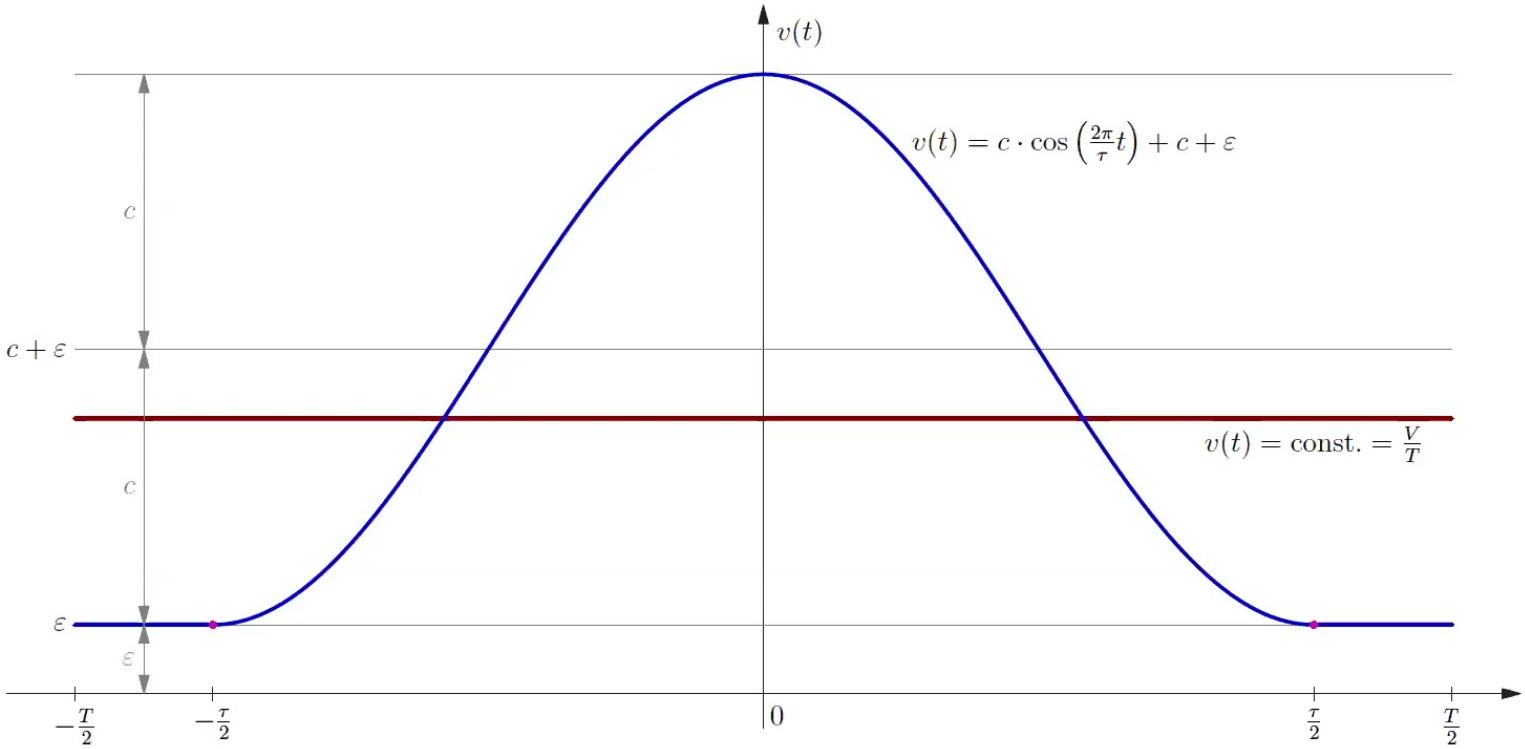

# Topology change

A scalar field with a strong enough jump ($\delta$) in a spatial direction introduces a *pinching* ($\varepsilon$), which results in an *effective* **change of spatial topology**.

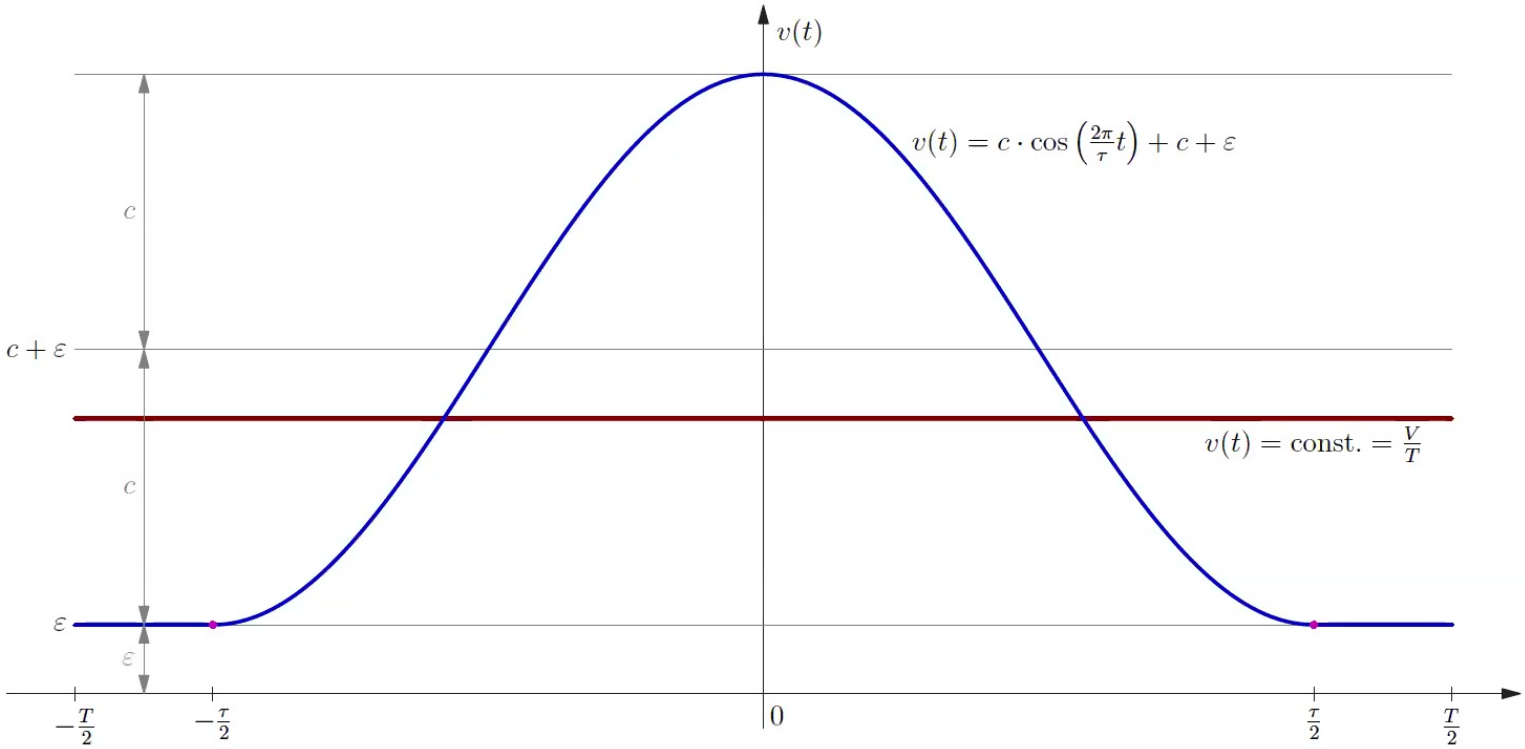

# Topology change

A scalar field with a strong enough jump ($\delta$) in a spatial direction introduces a *pinching* ($\varepsilon$), which results in an *effective* **change of spatial topology**.

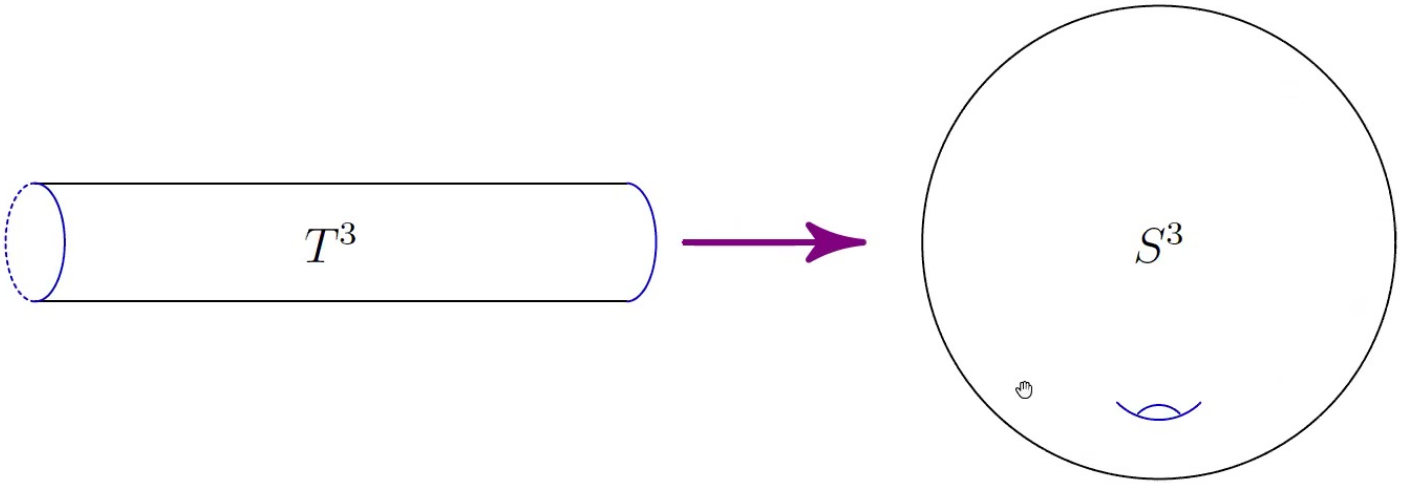

# Topology change

A scalar field with a strong enough jump ($\delta$) in a spatial direction introduces a *pinching* ($\varepsilon$), which results in an *effective* **change of spatial topology**.

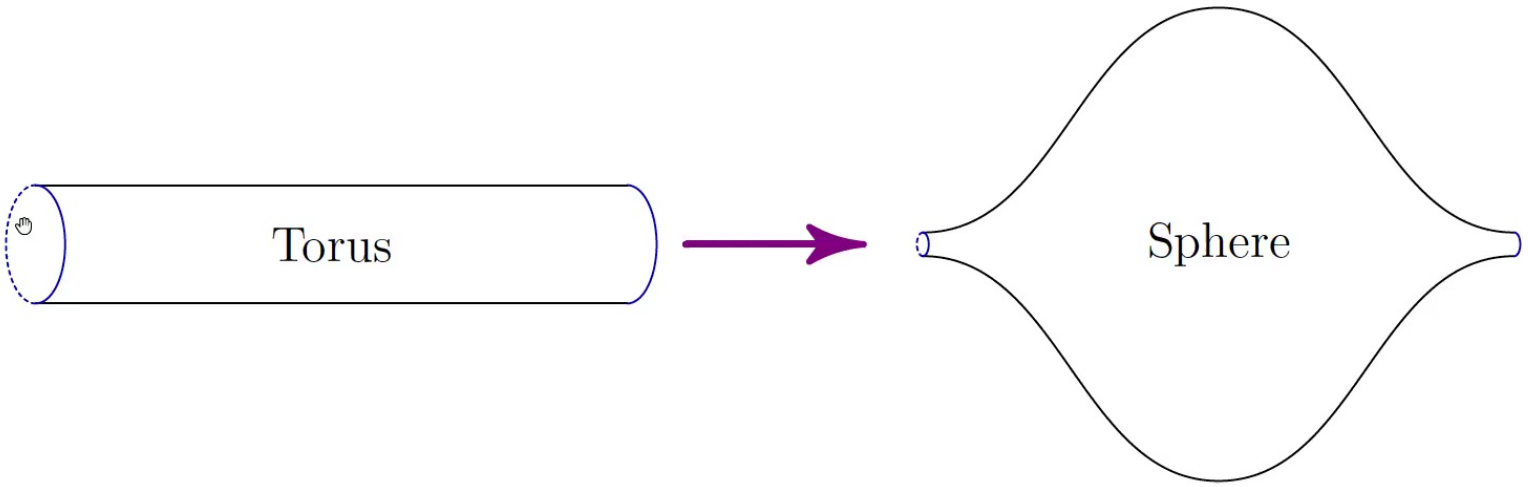

# Topology change

A scalar field with a strong enough jump ($\delta$) in a spatial direction introduces a *pinching* ($\varepsilon$), which results in an *effective* **change of spatial topology**.

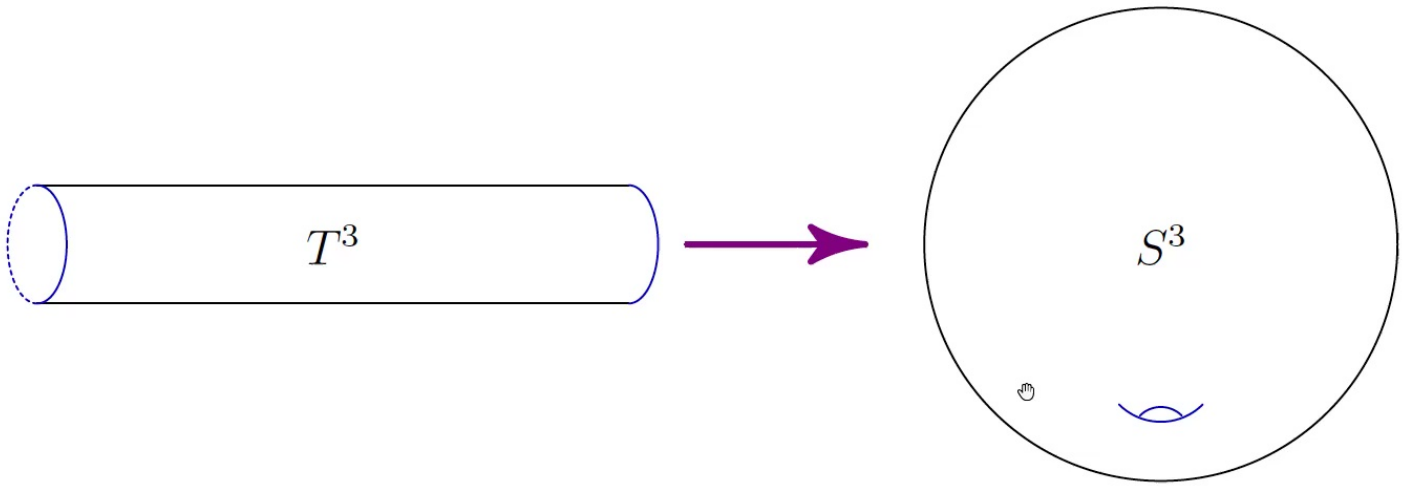

# Topology change

A scalar field with a strong enough jump ($\delta$) in a spatial direction introduces a *pinching* ($\varepsilon$), which results in an *effective* **change of spatial topology**.

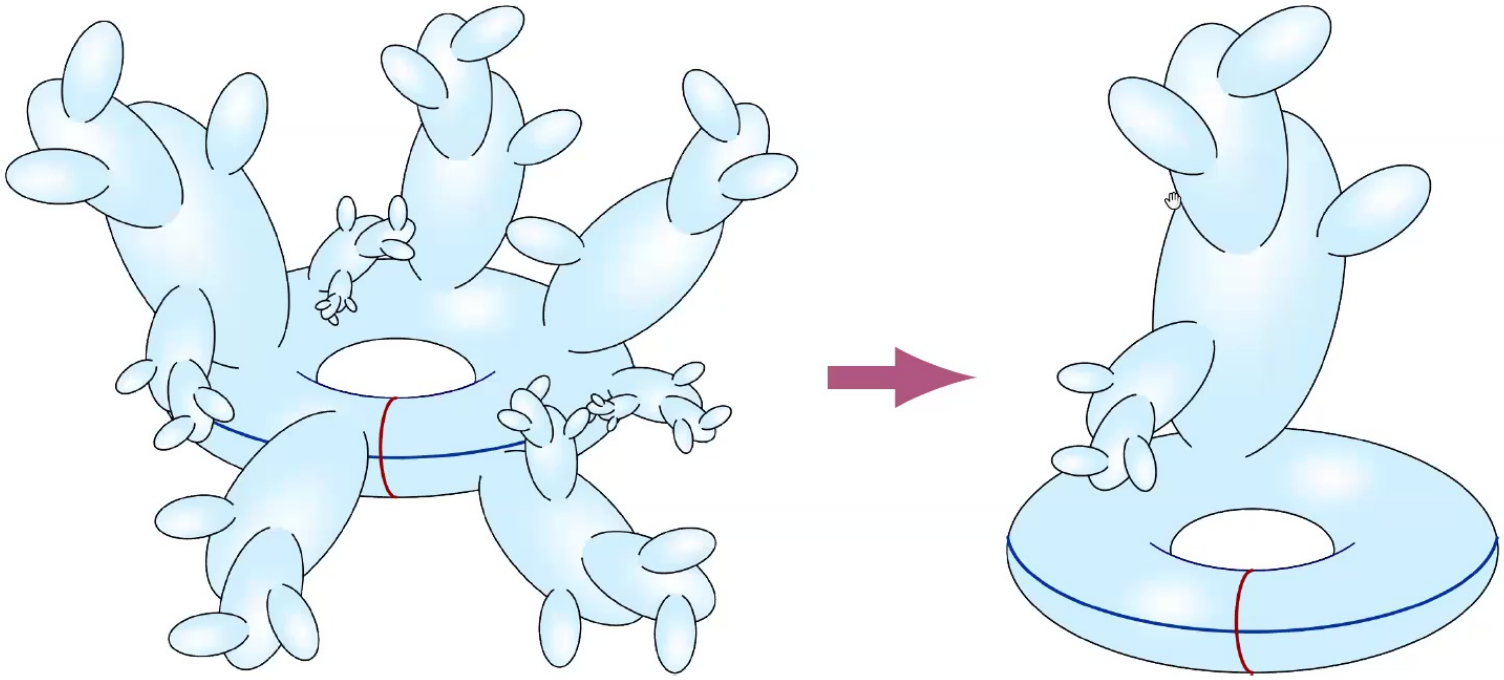

# Spherical vs toroidal spatial topology

Spherical ($S^3 \times S^1$) **Volume profile** Toroidal ($T^3 \times S^1$)

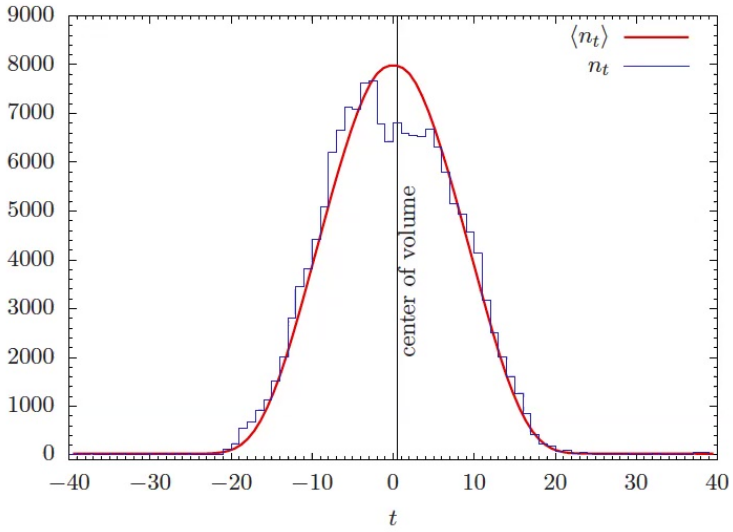


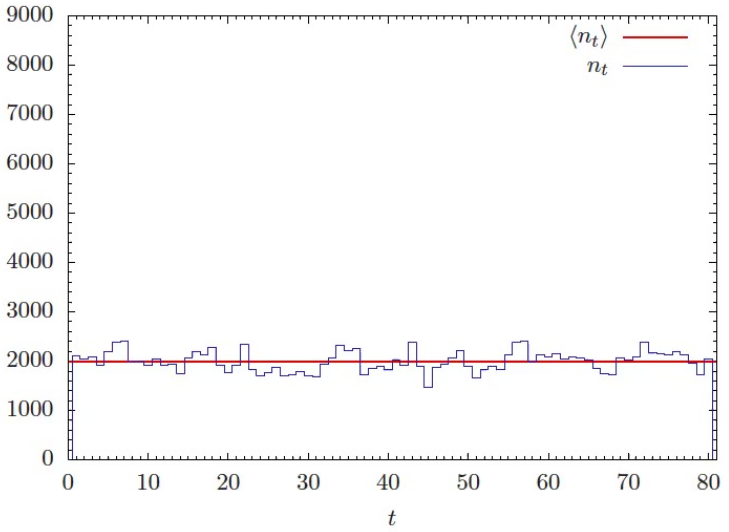


$$L[v] = \frac{1}{\Gamma}\frac{\dot{v}^2}{v} + \mu v^{1/3} - \lambda v$$
$$v(t) = a + b \cdot \cos^3(t/\tau)$$

$$L[v] = \frac{1}{\Gamma}\frac{\dot{v}^2}{v} + \mu v^{-3/2} - \lambda v$$
$$v(t) = \text{const.}$$

- Global proper-time foliation of spacetime manifold: $\mathcal{M} = \Sigma \times S^1$. The spatial leaves of foliation $\Sigma$ have a fixed topology.
- A difference between spherical and toroidal spatial topology is visible in the volume profile.
- It can be explained by the shape of the effective potential.

# Spherical vs toroidal spatial topology

Spherical ($S^3 \times S^1$) **Potential** Toroidal ($T^3 \times S^1$)

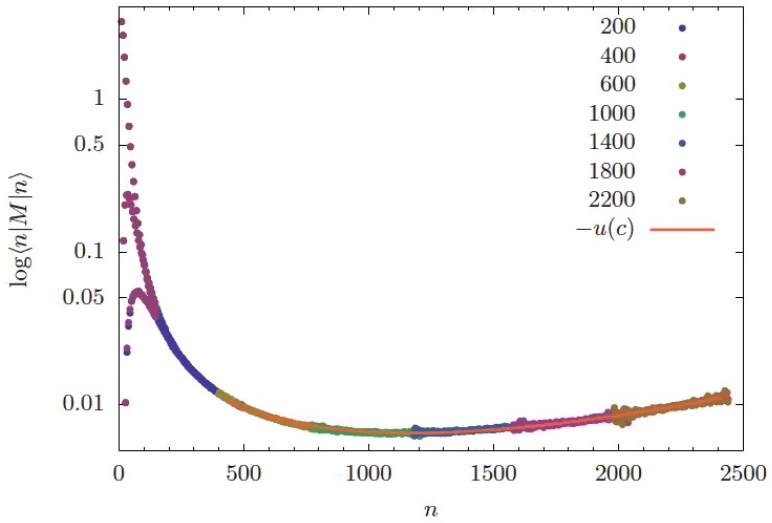


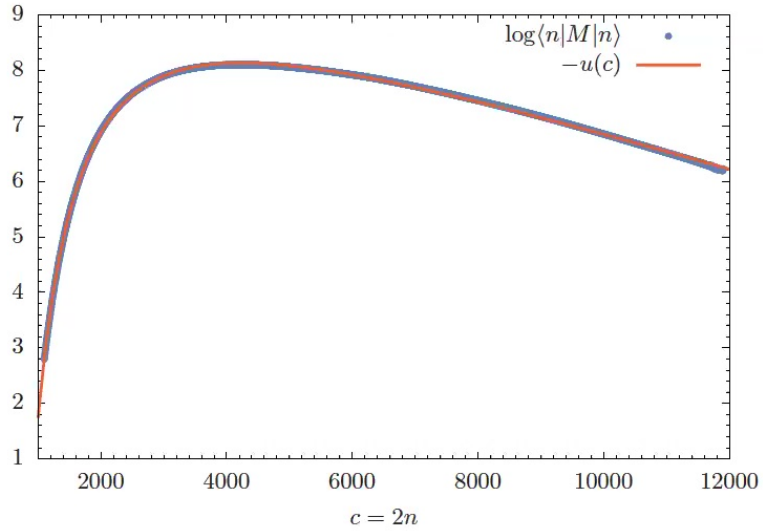


$$L[v] = \frac{1}{\Gamma}\frac{\dot{v}^2}{v} + \mu v^{1/3} - \lambda v$$
$$v(t) = a + b \cdot \cos^3(t/\tau)$$

$$L[v] = \frac{1}{\Gamma}\frac{\dot{v}^2}{v} + \mu v^{-3/2} - \lambda v$$
$$v(t) = \text{const.}$$

- Global proper-time foliation of spacetime manifold: $\mathcal{M} = \Sigma \times S^1$. The spatial leaves of foliation $\Sigma$ have a fixed topology.
- A difference between spherical and toroidal spatial topology is visible in the volume profile.
- It can be explained by the shape of the effective potential.

# Conclusions I

- *Causal dynamical triangulations* is a model of generic **geometry fluctuations at the Planck scale**.
- We introduced **coordinates** in spacetimes with toroidal topology via real classical **scalar fields** that span some interval and are invariant under boundary redefinition.
- To study **phase transitions**, we need an ensemble of **observables** which might shed some light on geometric fluctuations. Often, it is convenient to have a coordinate system at our disposal.
- **Fractal outgrowths** are visible as dense **clouds of points**.
- We observe a remarkable pattern of **voids and filaments**, which qualitatively looks quite similar to pictures of voids and filaments observed in our real Universe.

# Conclusions II

- Introduction of **dynamical scalar fields** with matching topological boundary conditions has a **dramatic effect on the geometries** that dominate the CDT path integral.
- This new kind of coupling between the topology of the matter fields and the topology of spacetime is likely to result in a **phase transition** for sufficiently strong coupling.
- The simple minisuperspace model predicts *a first order phase transition* as a function of $\delta$ for a jump in *time* direction.
- The classical limit agrees with *the minisuperspace model*.

# *Thank You!*

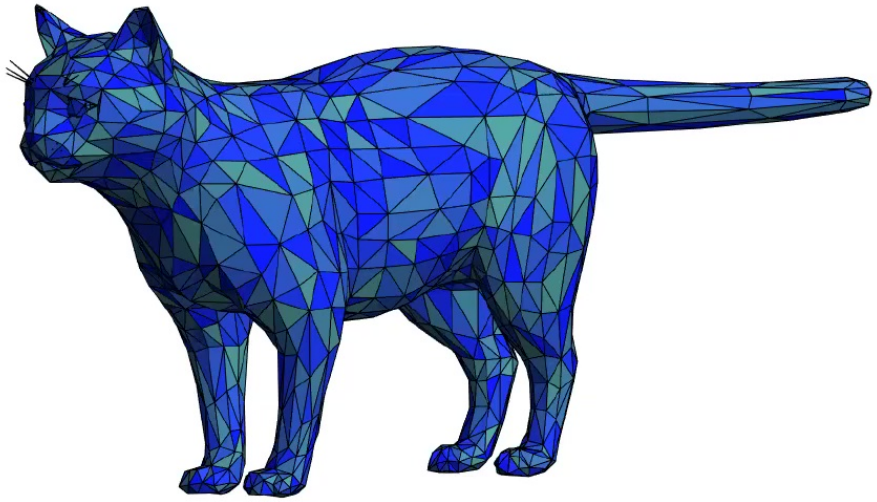

CDT Team in Kraków

Jerzy Jurkiewicz Jakub Gizbert-Studnicki Andrzej Görlich
Dániel Németh Zbigniew Drogosz

and

Jan Ambjørn